Medical University of South Carolina

MEDICA

MUSC Theses and Dissertations

2019

The Interaction Between Prpf8 and Dzip1 and its Role in Mitral Valve Prolapse

Janiece Sharmell Glover
Medical University of South Carolina

Follow this and additional works at: https://medica-musc.researchcommons.org/theses

Recommended Citation

Glover, Janiece Sharmell, "The Interaction Between Prpf8 and Dzip1 and its Role in Mitral Valve Prolapse" (2019). *MUSC Theses and Dissertations*. 210.
https://medica-musc.researchcommons.org/theses/210

This Thesis is brought to you for free and open access by MEDICA. It has been accepted for inclusion in MUSC Theses and Dissertations by an authorized administrator of MEDICA. For more information, please contact medica@musc.edu.

The Interaction Between Prpf8 and Dzip1 and its Role in Mitral Valve Prolapse

by

Janiece Sharmell Glover

A thesis submitted to the faculty of the Medical University of South Carolina in partial fulfillment of the requirements for the degree of Master of Science in Biomedical Sciences in the College of Graduate Studies.
Department of Regenerative Medicine and Cell Biology

2019

Approved by:

_____

Chairman, Russell (Chip) Norris

_____

Laura Kasman

_____

Antonis Kourtidis

_____

Robin Muise-Helmericks

Copyright Page

Dedication

This thesis is dedicated to my beloved family: my father, Fred, my mother, Marilyn and my sister Brittany, who fairly early on instilled in me that I could achieve anything I put my mind to! I would have never completed this journey without your constant support, love and prayers. Thank you for believing in me and feeding me words of encouragement in times of need.

Acknowledgements

First and foremost, I want to give all the honor and glory to my Lord and Savior, Jesus Christ. Without you, none of this would have been possible. Thank you for the strength to endure it all. All things are possible because of Him. Second, I want to thank my family and friends for always supporting me in all my endeavors. I would also like to thank The Medical University of South Carolina and the Master of Biomedical Science Program for this amazing opportunity to further my education. I would also like to acknowledge my committee members. Chip, my mentor, thank you for your leadership and patience throughout this process. I appreciate you taking me under your wing and teaching me the rules of the trade. Your guidance has truly shaped me into the scientist I am today and I am forever grateful. Dr. Kasman, thank you for your endless words of encouragement and directivity throughout my graduate school journey. Dr. Kourtidis, thank you for your constant support and uplifting attitude. Thank you, Dr. Muise-Helmericks for your creative ideas and driving me to think independently! I am a better scientist because of all of the time and effort you all poured into me over the past year. Finally, thank you to all the members of #norrislab, Kate, Diana, Lilong, Kelsey, Rebecca, Reece, and Mary-Kate your wisdom and encouragement has undoubtedly pushed me to the finish line.

This project was funded by: National Heart Lung and Blood Institute: 5P20 GM103444-07; National Heart Lung and Blood Institute: 1R01 HL131546-01A1; American Heart Association: 11SDG5270006; Leducq Foundation 07CVD04

TABLE OF CONTENTS:

LIST OF FIGURES

LIST OF TABLES

LIST OF ABBREVIATIONS

3C-Chromatin Conformation Capture
ATF-Adult Tail Fibroblasts
AV-Atrioventricular
BD- Barlow's Disease
BMP- Bone Morphogenetic Protein
CRISPR-Clustered Regularly Interspaced Short Palindromic Repeat
CVD-Cardiovascular Diseases
DCHS1-Dachsous Cadherin- Related 1
DZIP1-DAZ Zinc Finger Protein 1
ECL- Enhanced Chemiluminescence
ECM- Extracellular Matrix
FED- Fibroelastic Deficiency
GLI3-GLI Family Zinc Finger 3
GLIS2- GLIS Family Zinc Finger 2
GWAS-Genome Wide Association Study
HDF-Human Dermal Fibroblasts
HEK293T-Human Embryonic Kidney Cells
Hh-Hedgehog Signaling
IFT88-Intraflagellar Transport Protein 88
IHC-Immunohistochemistry
MVP-Mitral Valve Prolapse
OFT- Outflow Tract
PDGFRa-Platelet-Derived Growth Factor Receptor Alpha
PKD-Polycystic Kidney Disease
PRPF8-Pre-mRNA Processing Factor Protein 8
RNASeq-Ribonucleic Acid Sequencing
RT-Reverse Transcription
SL- Semilunar Valves
SNP- Single Nucleotide Polymorphism
TBST-Tris Buffer Saline-Tween
VIC- Valvular Interstitial Cells
VEC- Valvular Endothelial Cells
Wnt-Wingless/Integrated
XMVD- X-linked myxomatous valvular dystrophy
Y2H- Yeast 2-hybrid

JANIECE SHARMELL GLOVER, The Interaction Between Prpf8 and Dzip1 and its Role in Mitral Valve Prolapse (Under the direction of RUSSELL A. NORRIS)

ABSTRACT

Mitral Valve Prolapse (MVP) is one of the most common cardiac diseases affecting 1 in 40 individuals worldwide. Functionally, MVP is the abnormal billowing of one or both of the mitral valve leaflets into the left atrium during ventricular systole. Structurally, the valves experience an accumulation of proteoglycans, an increase of collagen and hyperplasia. An echocardiogram can be used to diagnose the disease as well as determine the severity of it. MVP can cause several underlying effects such as regurgitation, arrhythmias and even sudden cardiac death in severe cases. Although there is very little known about the cause of the disease, recent discoveries have identified various genetic associations with MVP. This is the basis by which we structure this proposal.

A linkage analysis was conducted on a large family with non-syndromic MVP to find a common cause for the disease. Through this linkage analysis a specific region of genes was identified, in particular, a cilia gene, *DZIP1* was found along with the point mutation in the gene. Through expression, knockout studies and biochemical approaches we have gained a better understanding of what *DZIP1* and the mutation of $DZIP1^{S14R/+}$ are doing during cardiac development. Currently, little is known about how mutations in the cilia gene can influence the development of MVP. To address this question, a two-hybrid screening was completed, in which *DZIP1* wild type plasmid and mutant DZIP1 plasmid were used to determine *DZIP1*'s binding partners.

A pre-mRNA processing factor protein named Prpf8, which is a fundamental component of the spliceosome, was found to interact with the wild type DZIP1 plasmid but was the only protein found to not interact with the mutant DZIP1 plasmid. Additionally, the previous GWAS completed on patients with MVP identified a single nucleotide polymorphism (SNP) in close proximity to the PRPF8 locus, which led us to hypothesize that this SNP could function as an enhancer to regulate Prpf8 expression. Here we present data that shows that Prpf8 is expressed in the mitral valves at various embryonic and postnatal stages, and that it co-localizes with DZIP1. Verification of the two-hybrid screening result was tested through co-immunoprecipitation from protein collected from wild type ($Dzip1^{+/+}$) and mutant ($Dzip1^{S14R/+}$) adult mouse tail fibroblasts.

Furthermore, through collaborators at INSERM, chromatin conformation capture experiments on chromosome 17 (where PRPF8 is located) determined four potential regulatory sequences that are in close proximity to PRPF8's transcription start site. With the given data, luciferase assays indicated sequences with enhancer function. The studies presented will establish a broad mechanism by which DZIP1 mutations regulate RNA splicing, resulting in myxomatous valves and MVP in patients.

CHAPTER 1: INTRODUCTION AND BACKGROUND

Introduction

The heart marks the center of the circulatory system. It is comprised of four chambers: the left atrium, right atrium, left ventricle and the right ventricle. Each component of the heart plays an important role in governing how efficiently blood flows through it to keep a living organism alive and well. The left and the right side of the heart have their own pumping systems but communicate effectively. The right atrium is responsible for receiving deoxygenated blood from the body and pumps it to the right ventricle through the tricuspid valve. The right ventricle then pumps the deoxygenated blood to the lungs through the pulmonary valve. In contrast, the left atrium receives the oxygenated blood from the lungs and pumps it to the left ventricle through the mitral valve. Finally, the left ventricle pumps the oxygen-rich blood through the aortic valve out to the rest of the body (Buckberg, Nanda, Nguyen, & Kocica, 2018).

Our lab is interested in heart development and how improper heart development can lead to cardiac disease in a patient's life. More specifically, we focus on cardiac valve development. As mentioned earlier there are four valves within the heart: the pulmonary valve, the aortic valve, the tricuspid valve and the mitral valve. All serve to promote unidirectional blood flow throughout the heart. If there is any disruption to this process, for example, incorrect valve development, this can lead to valve disease like mitral valve prolapse. My research aims to establish a mechanism by which the heart disease, mitral valve prolapse begins. This is pertinent to recent studies because it also provides a starting point for understanding the fundamental molecular and developmental processes that can be applied to the disease in general. The following chapters will

address our recent developmental, genetic, and molecular discoveries behind valvular development and mitral valve prolapse.

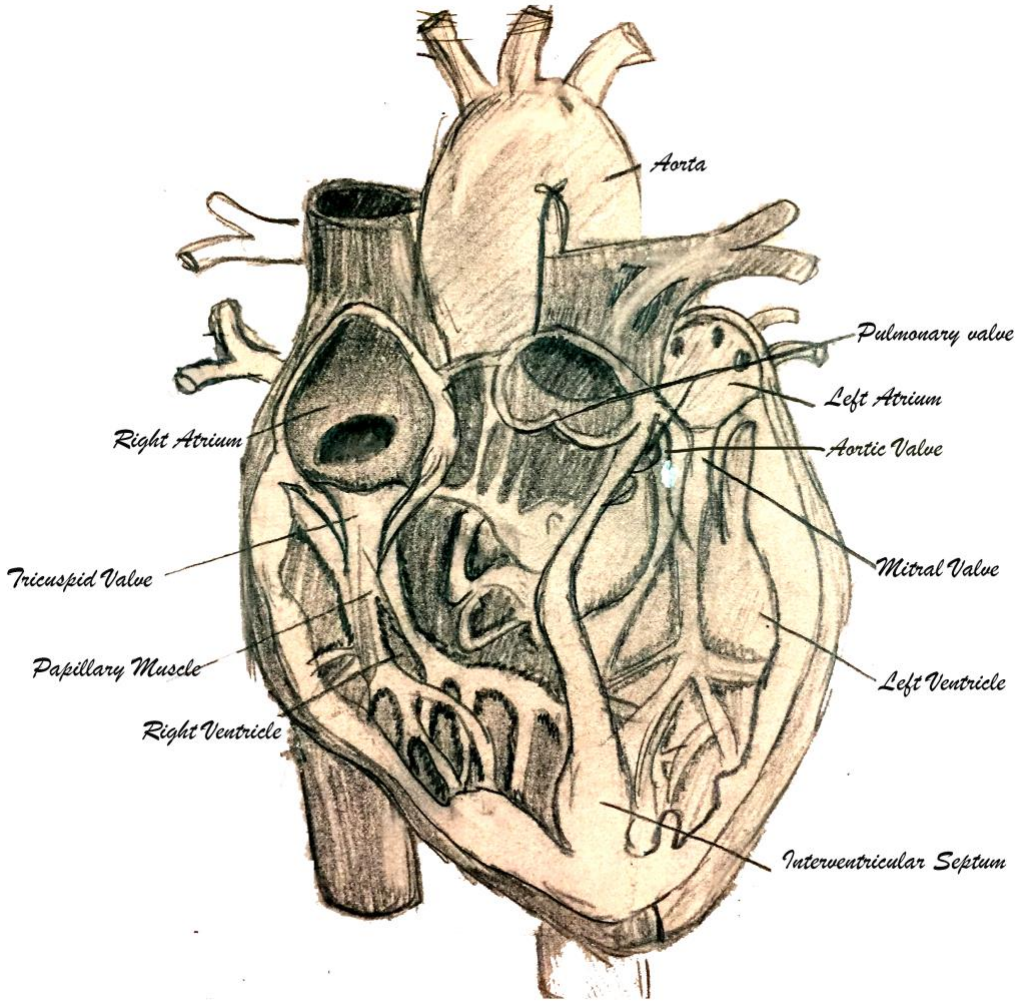

Figure 1.1 The Gross Anatomy of the Human Heart. The human heart is comprised of four chambers: the left atrium, right atrium, left ventricle and the right ventricle. The left and the right side of the heart have their own pumping systems. The right atrium receives deoxygenated blood from the body and pumps it to the right ventricle through the tricuspid valve. The right ventricle then pumps the deoxygenated blood to the lungs through the pulmonary valve. The left atrium receives the oxygenated blood from the lungs and pumps it to the left ventricle through the mitral valve. The left ventricle pumps the oxygen-rich blood through the aortic valve out to the rest of the body (Drawing by Rebecca Stairley, Norris Lab).

Valve Development

The human heart consists of four chambers (right atrium, right ventricle, left atrium and left ventricle), and four valves (aortic and pulmonic semilunar (SL), mitral and tricuspid valves). For the purpose of this study, we focus on the mitral valve leaflets. The mitral valve leaflets are positioned directly between the left atrium and the left ventricle. The structure of the leaflets, plays an important role for proper function. (Figure 1.1). The valves work together to maintain unidirectional blood flow throughout the heart and are responsible for opening and closing over 100,000 times a day. (Horne et al., 2015). The mitral valve leaflets are enclosed with endocardial endothelial cells, while the remaining volume of the leaflet is made up of valvular interstitial cells (VICs) (Hinton et al., 2006; Rabkin-Aikawa, Farber, Aikawa, & Schoen, 2004)

Valve development initiates from a cardiac tube that is comprised of myocardium and endocardium. Between these two cell layers is a region called the cardiac jelly which is comprised of space-filling proteoglycans (Person, Klewer, & Runyan, 2005). The myocardium secretes various growth factors which induce the endothelium to undergo endothelial-to-mesenchymal transformation (EMT). This results in the cardiac jelly being invaded by mesenchyme to initiate the first phases of valve development. This process is extremely crucial in defining correct valve formation. As the valves continue to grow and stretch further into the left ventricle, the fibrous leaflets become thinner, increasing the extracellular matrix (ECM) deposition and remodeling. It is not until days after the birth of a newborn, that highly organized and distinct layers that represent the ECM are seen. The ECM of the valve is composed of three stratified layers that are rich in collagens, proteoglycans and elastin. Both mouse and human valves have these

boundaries although there is slight variation on how many ECM zones exist. The complete valve maturation and remodeling in mammals will continue into juvenile stages. (Combs & Yutzey, 2009).

Over the years there have been many studies that have included the similarities between animal models and human anatomy, in order to make new discoveries in translational science. Therefore, the comparison of adult aortic valve leaflet structure and composition demonstrates similar stratification in humans, sheep, chickens, rabbits, and mice (Combs & Yutzey, 2009). The process of valve formation has certainly been universal over time, accommodating the species in which they reside. For example, even in the smallest of species we see conserved valve cell regulatory mechanisms being represented in *Drosophila* (Lammers et al., 2017).

As we examine valve formation on a molecular level we look to evaluate the endocardial cushion composition and how the study of valve development includes different signaling mechanisms. The first studies that identified EMT in the heart were through pioneering work from the laboratory of Roger Markwald (Markwald, Fitzharris, & Manasek, 1977). When chick cardiac explants were placed on a collagen lattice, the endocardium was seen adopting migratory and invasive characteristics. However, when the myocardium was removed from these cultures, the endocardium failed to change its phenotype. This was the first evidence demonstrating that myocardial-secreted factors could induce an endothelial-to-mesenchymal transformation. From these seminal studies, concerted efforts have focused on identifying the myocardial initiating signals (Runyan & Markwald, 1983). Since then, major growth factors have been identified that regulate this EMT process, such as transforming growth factor beta (TGFb) and basic metabolic panel

(BMP). Notch signaling, active in the endocardium, has also been defined as playing a critical role in EMT progression and can synergize with TGFb and BMP ligands (Garside, Chang, Karsan, & Hoodless, 2013). The endocardial-to-mesenchymal transition process occurs when subsets of AV (atrioventricular) and OFT (outflow tract) endocardial cells transform into a mesenchymal phenotype, which determines the anatomical placement where the valves will form within the primary heart tube (de Vlaming et al., 2012).

Additionally, the process of valve development occurs in various steps. These steps include: the formation of the ECM, the migration of endocardial cells into the ECM, the event of cardiac looping that induces endocardial cushion swellings, triggering the overpopulation of endocardial cushions (Markwald, Fitzharris, Bolender, & Bernanke, 1979) (Eisenberg & Markwald, 1995) and the eventually forming the stratified layers (proteoglycans, elastin and collagen) of the ECM (Figure 1.2). Additionally, the cause of the swelling results from the myocardium of specific regions of the primary heart tube, the AV junction and the OFT upregulates the secretion of the ECM. This process gives rise to cushion morphogenesis induces a subset of AV and OFT endocardial cells to lose their junctions and adopt a mesenchymal-like phenotype as they migrate into the cardiac jelly (Person et al., 2005). Furthermore, there have been studies that state the role that both myocardial and endocardial- derived signaling pathways affect endocardial cushion EMT and proliferation of valve progenitor cells (de Lange et al., 2004). Eventually, this forms the division between the myocardium and the endocardium.

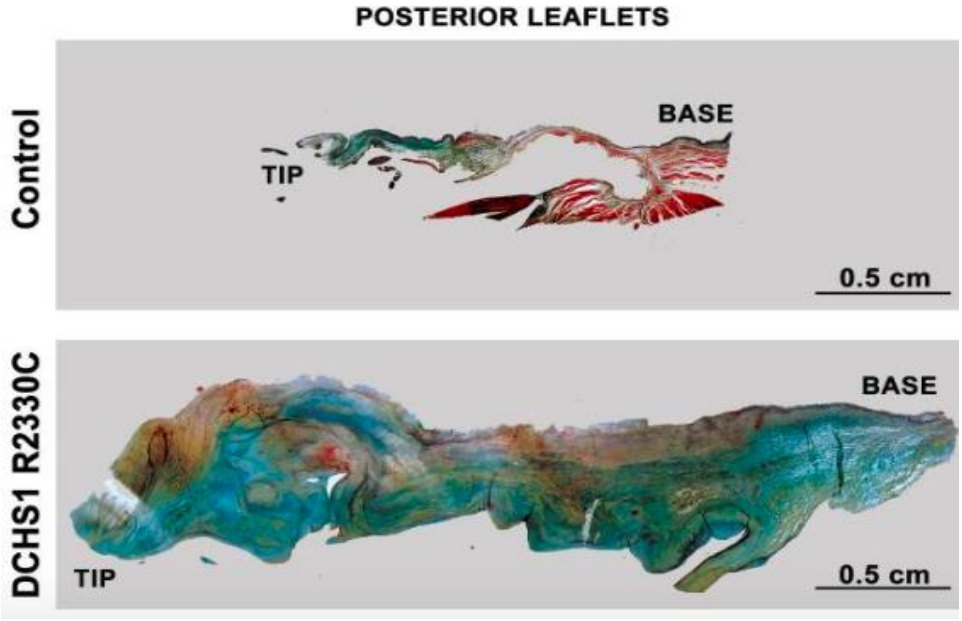

Figure 1.2 Myxomatous Degeneration in Valves. Human posterior leaflets of control and DCHS1 p.R2330C were isolated, fixed and stained with Movats Pentachrome. Leaflet thickening, elongation and myxomatous degeneration is observed in the DCHS1 p.R2330C leaflet compared to control. Expansion of the proteoglycan layer (blue) and disruption of the normal stratification of matrix boundaries is observed in DCHS1 p.R2330C leaflets. Blue=proteoglycan, Yellow=collagen, Black=elastin, Red=fibrin or cardiac muscle. Scale bars = 0.5cm (Durst et al., 2015).

Cell Types in the Mature Mitral Valve

Through the previous events of valve development, the valve becomes mature and has its own different cell types. There are two main cell types that make up the valves. Those are the valvular interstitial cells (VICs) and the valvular endothelial cells (VECs). The VEC's reside on the outer rim of the leaflets, creating a border for the valve. It has been shown that any infiltration or breakage of this border can lead to valve disease (Butcher & Nerem, 2007) (Leask, Jain, & Butany, 2003), (Butcher & Markwald, 2007) (El-Hamamsy et al., 2009).

The majority of each leaflet is composed of VIC's. Their fibroblastic consistency aids in several different characteristics throughout the valve, due to their various placements within the leaflets (Horne et al., 2015). The VIC's essentially act as first responders: if given enough stress they have the capability of migrating and contracting, rather than staying in their resting state. Their main role is to mediate and maintain the ECM structure, throughout the maturation of valve development. Any disturbances in the roles of either of these cell types can lead to unfavorable consequences that can affect the biomechanical functions leading to diseases. The overall progression of valve development has many evolving steps and, in any event, if there is a misstep in the process there will be severe complications.

Biomechanical Influences

As the valve is undergoing maturation, additional factors can play a role on how the valves are able to perform their job accurately, for example biomechanical forces. In a fully developed heart the act of blood flowing from the atrium to the ventricle represents blood going from an area with low pressure to an area that is high in pressure. Previous

studies have stated that the biomechanical forces behind effectively beating the heart during valve development influence the formation and matrix composition of the valves (Butcher, McQuinn, Sedmera, Turner, & Markwald, 2007). Specifically, during isovolumetric relaxation, which is an interval in the cardiac cycle, the pressure difference between the left atrium and the left ventricle causes the MV leaflets to open and allow blood to flow from the left atrium into the left ventricle during diastole (Giovanni et al., 2017). During this time the left ventricle stays in a relaxed state, allowing it to maintain a positive transmitral pressure and aids in filling the ventricle without complications. Soon after active ventricular relaxation, the fluid begins its deceleration and the MV partially closes, preventing any backflow of blood into the atrium (Sagie et al., 1994).

Additionally, the leaflets of the mitral valve are connected to tendinous chords, which attach to the left ventricular myocardium through the papillary muscle. These fibrous structures provide tension to the mitral leaflets, this along with several other mechanical systems at play keep the tissues from ballooning upward into the left atrium during ventricular systole. Furthermore, *in vitro* models have suggested that vortices, the region of blood that is fixed around an axis line, is crucial to the closing of the valve. These vortices are generated by ventricular filling and aid the partial closure of the MV following early diastole and are essential for the closing of the valve. Without these vortices, the valve would not be able to close during ventricular contraction (Bellhouse & Reid, 1969).

Developmental Basis of Disease

As a basis to start investigating valve disease, researchers have designed many studies surrounding genetic disorders found in large families and from previous work

published on the matter. It has been stated that scientists find similarities in diseases like Alzheimer's and diabetes because of the similar genetic anomalies surrounding these diseases and valve disease. In each instance there are gene mutations, these mutations are present at conception, this leads to inheritable traits passed from generation to generation in families and the diagnosis of these diseases appearing later in life. Identifying the genes and their function in familial disease is vital in understanding how mutations of these genes lead to disease. With mitral dystrophies, individuals in a family can show a high degree of variation in when they are diagnosed with the disease, despite the fact that the affected individuals all carry the same mutation. It has been found that children with clinically relevant mitral valve prolapse (MVP) have been diagnosed as young as six years of age. In these families, mutations in the Filamin-A result in familial cardiac valvular dystrophy (Kyndt et al., 1998). Furthermore, this knowledge proposes that a patient's genetic makeup accompanied with genetic variants that are present at the time of valvulogenesis, could dictate the severity of the valve disease. This knowledge is key in investigating the complexity behind valve disease, as it could open the door for new therapeutic aids and the discovery of associated pathways that are required for proper valve development.

Mitral Valve Prolapse

MVP is the most common form of cardiac valve disease and is a major health burden. The disease is characterized by the abnormal billowing of one or both of the mitral valve leaflets. Structurally the disease causes myxomatous degeneration and the valves experience an increase in proteoglycan accumulation, fragmented collagen and hyperplasia. This phenotype prevents the valve from functioning properly. This also

causes an imbalance of biomechanical forces that affects the correct positioning of the leaflets as well.

This disease affects 1 in 40 people worldwide, making its prevalence rate between 2-3%. Based on this information, MVP is expected to afflict approximately 176 million people worldwide (Devereux et al., 1987). These staggering numbers have brought much needed attention to this disease, yet there are many factors surrounding MVP that are unknown. The term, MVP was coined Barlow in 1963 (Barlow & Pocock, 1963) when he detected mitral regurgitation in the one of his patients when examining their heart through an angiography. MVP carries a significant burden of morbidity and mortality. There are no effective nonsurgical treatments for MVP and an incomplete understanding of its fundamental causes has hindered therapeutic efforts. While surgical techniques continue to improve, the number of surgical cases and associated mortality rates are increasing. Surgeries for degenerative mitral valve disease increased by more than 44% from 2011-2016 and, currently >90,000 mitral valve surgeries occur each year making it the fastest growing cardiovascular intervention in the United States (Coutinho & Antunes, 2017). MVP can lead to arrhythmias, heart failure, and even sudden cardiac death and 1 in 10 patients will require valve surgery. Through various studies it was found that MVP could be inheritable or naturally irregular, but the initial diagnosis of MVP left many patients undetected.

The Framingham Heart study detailed vital information found in the echocardiography of MVP patients. It was found that echocardiographers misinterpreted the phenotype because positioning of echo probe did not relay proper mitral valve geometry (Freed et al., 1999). Initially, the physicians were doing an apical view to

obtain the correct orientation of the valve. Yet, when probe was turned there was accurate representation of the myxomatous valve. Through this study physicians were able to develop a more efficient and precise way to diagnosis MVP patients and also detect accompanying health defects with this disease like heart failure and atrial fibrillation.

Recent genetic studies by our group have provided new hope in identifying MVP disease mechanisms, as we were the first to describe genetic causes for non-syndromic MVP (Durst et al., 2015) (Dina et al., 2015) (Figure 1.3). Furthermore, through these genetic studies our lab has linked primary cilia with MVP (Durst et al., 2015) (Dina et al., 2015). In this study we have used this information to develop testable hypotheses that will uncover key mechanistic insights into MVP pathogenesis at a cellular and molecular level.

Table 1.1: Genes associated with MVP. Genetic anomalies associated with mitral valve prolapse in humans. (Durst et al., 2015) (Dina et al., 2015) (Kyndt et al., 1998) (Le Tourneau et al., 2018).

Table 1.1 Genetic associations with mitral valve prolapse in humans

	Gene or chromosome	**Defect localization/mechanism/Phenotype**
Non-syndromic MVP		
Filamin A-MVD	*FLNA*	Mechanotransduction/ Cardiac valvular dystrophy
Myxomatous disease (MMVP2)	*DCHS1*	Cell Migration and polarity/ *Dchs1* mutations = MVP
Myxomatous disease (MMVP1-3)	*Chr 16-13*	--
Frequent Variants GWAS	*LMCD1*	Transcription factor/ Knockdown of LMCD1 in mice= valve regurgitation
	TNS1	Focal adhesion protein/cytoskeleton organization/*Tns1*$^{-/-}$ mice= myxomatous degeneration in posterior leaflet

Cilia as a Focus

Due to our genetic discoveries in MVP patients that revealed a preponderance of mutations in cilia genes, we choose to focus on how these gene variants may affect ciliogenesis. Cilia are microtubule-containing structures (axonemes) that project from the cell. There are two main types of cilia: motile and immotile. Whereas motile cilia (>100/cell) are largely used to move fluid or gametes, immotile cilia (a.k.a. primary cilia) are solitary (typically one per cell), extend from the centriole/basal body and were previously thought to be vestigial evolutionary remnants with no persisting function. However, this traditional belief was challenged by recent genetic discoveries that linked mutations in cilia genes to a spectrum of rare syndromic diseases known as ciliopathies. These findings spurred concerted efforts to understand ciliogenesis, their downstream pathways, as well as additional genetic conditions that stem from defects in cilia structure and/or function. MVP (Durst et al., 2015). What is emerging from these studies is that primary cilia function as transducers of mechanical, electrical and chemical signals in a tissue-specific and temporal-dependent context. In doing so, they relay information regarding various growth factor signals including Hh, Wnt and Pdgfa to influence cell survival, differentiation, and tissue organization. How cilia are built (aka ciliogenesis) is still poorly understood, but critical for uncovering novel etiological underpinnings for MVP.

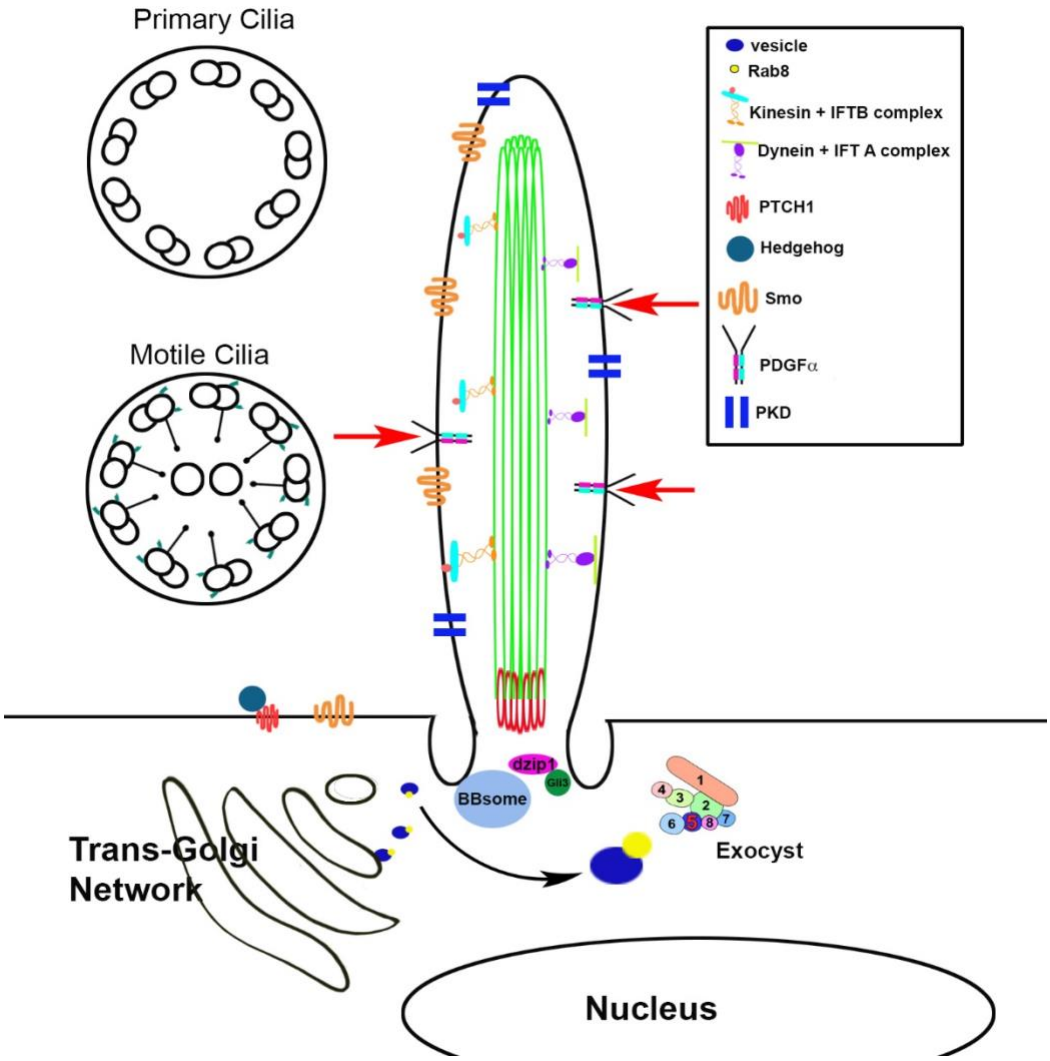

Figure 1.3 Primary Cilia Governs the Signaling Pathways for the Cell.

Primary cilia and motile cilia are essential for many common signaling pathways. Primary cilia exhibit a 9+0 microtubule ratio and in contrast motile cilia have a 9+2 ratio. Primary cilia are one per cell and act as mechanosensors of fluid flow and contribute to cell-cell communication (Image by Diana Fulmer, Norris Lab).

CHAPTER 2: IDENTIFYING THE INTERACTION BETWEEN DZIP1 AND PRPF8

Introduction

MVP is one of the most common cardiac diseases and it is the most common cardiac valvular disease. MVP can occur as part of a recognized syndrome such as Marfan syndrome, characterizing it as syndromic MVP, or it can occur in isolation in which case it is called non-syndromic MVP. Although genetic causes for some syndromic forms of MVP are known, the genetic underpinnings of the more common non-syndromic form of MVP, which affects 2-3% of the population, have remained elusive. MVP occurs when the mitral valve leaflets disrupt steady blood flow from the left atrium to the left ventricle. This happens when either one or both of the leaflets (posterior and anterior) balloon upward into the left atrium.

Through the findings revealed in the Framingham Heart study, the diagnosis of MVP was fully understood and scientists took a closer look into the genetics behind the disease. In 1999, researchers performed familial screens that identified the first locus associated with autosomal dominant MVP, MMVP-1. The locus is on chromosome 16p (Disse et al., 1999) and by performing several more screens that verified the heterogeneity of the disease, linkage analysis mapped to two loci. This was followed by more studies linking MMVP2 located on chromosome 11p15.4.

Additionally, in 2007, the gene Filamin A was found to be linked to MVP because the of its involvement in X-linked myxomatous valvular dystrophy (Le Tourneau et al., 2018; Toomer et al., 2019). These studies ignited researchers to delve more into this finding and search for more components that are responsible for MVP in patients. We now have compelling genetic and functional evidence that significantly advance our understanding of MVP pathogenesis. The gene *DCHS1* (Durst et al., 2015) is well-

known for its encoding of calcium-dependent cell-cell adhesion molecules. Previous studies within our lab found that mutations in DCHS1 cause MVP. Additionally, a genome-wide association study has led many scientists and healthcare professionals to observe genetic variants within these MVP patients (Dina et al., 2015). However, patients with rare syndromic diseases that stem from alterations in the structure and function of primary cilia ("ciliopathies") have a higher prevalence of MVP, suggesting that primary cilia may play a broad role in disease etiology.

Results

Genetic studies

To date, there has been a short list of genes that are implicated in MVP, some of which are: *DCHS1, TNS1 and LMCD1*. Specifically, *DCHS1* mutations causes myxomatous valves and has been linked to polycystic kidney disease (PKD), which is another ciliopathy (Durst et al., 2015). In a previous GWAS, where 6 significant loci in association with MVP were found, genes *TNS1* and *LMCD1* showcased phenotypes linked to MVP. *Tns1*$^{-/-}$ mice exhibit an enlarged posterior leaflet and the knockdown of *LMCD1* in mice led to valve regurgitation (Dina et al., 2015). The connections made through investigating these genetic associations would lead to more inheritable findings in MVP patients.

Furthermore, we studied the pedigree of a family with non-syndromic MVP we began to identify crucial players involved with the disease. Using a combination of linkage analyses, as well as exome and capture sequencing, we recently identified loss of function mutations in the cilia gene, *DZIP1,* that segregate with mitral valve prolapse in multiple MVP families. Dzip1 is a centrosomal protein that is required for ciliogenesis.

Patients with *DZIP1* missense mutations displayed autosomal dominant inheritance, which we have shown in multiple model systems to cause haploinsufficiency and disease phenotype, making *DZIP1*, a novel gene for mitral valve prolapse. As we begin to examine the connections between primary cilia and MVP we take a closer look for the expression of primary cilia during valve development.

Temporal Expression of Primary Cilia Through Valve Development

To determine whether primary cilia is expressed on the mitral valves immunohistochemical stains were completed, by marking the basal body (gamma tubulin) and the axoneme (acetylated tubulin). These stains were imaged using high-resolution confocal microscopy. Through this application we observed the expression of cilia on early embryonic stages of valve development (E13.5-E15.5), specifically on the valvular interstitial cells (VICs). Primary cilia are noticeably absent on the valvular endothelial cells (VECs) and begin to digress in expression at timepoints after postnatal day 0 (Figure 2.1). Through examining the localization of primary cilia, we begin to expose their role in valvular development.

As mentioned earlier we see an influx of primary cilia being expressed on all cells during early stages of development, particularly the VICs. When the ECM is beginning to form it is mostly composed of proteoglycans like versican and through development the stratified layers begin to appear. It is noted that primary cilia are more co-localized to areas that are rich in proteoglycans (Figure 2.2). This discovery gives insight on the expression pattern of primary cilia as they are seen through valve development. Furthermore, applying the information known about biomechanical forces being a key player in having proper valve development, research suggests that primary cilia are able

to sense the change in blood flow and adapt to this change by acting as mechanosensors to regulate valvulogenesis. Even though this function of primary cilia is still not fully understood, there have been efforts toward this possibility (Nauli et al., 2013) , each study giving us more insight on the role cilia play in valve development.

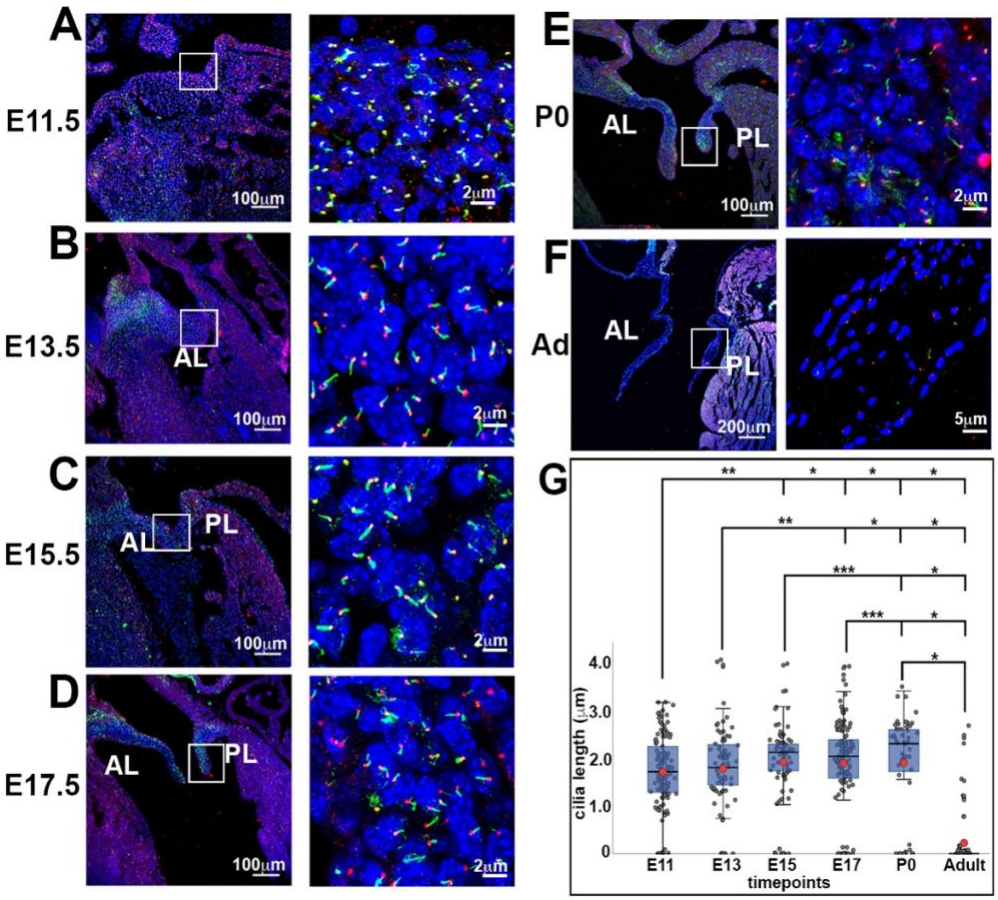

Figure 2.1 Localization of Primary Cilia During Mitral Valve Development. (A-F) IHC performed on wild type mouse heart tissue. Co-staining of the axonemes (green, acetylated a-tubulin) and the basal bodies (red, g-tubulin) show cilia expressed on murine mitral valve interstitial cells but not on valve endocardial cells at these stages. Blue=Nuclei (Hoescht), AL, PL = Anterior and Posterior Leaflets, respectively. **(G)** Box plot of cilia lengths in the mitral valves showing growth in length during development with few cilia observed in the adult valve. The blue boxes show the main distribution of the cilia length values. The bottom of the box is the 25th percentile, the middle line is the median value, and the top of the box is the 75th percent. Red dot denotes the mean cilia length. Error bars represent 95% confidence intervals. *=$p < 0.0001$, **=$p < 0.001$, ***=$p < 0.01$ (Image by Diana Fulmer, Norris Lab).

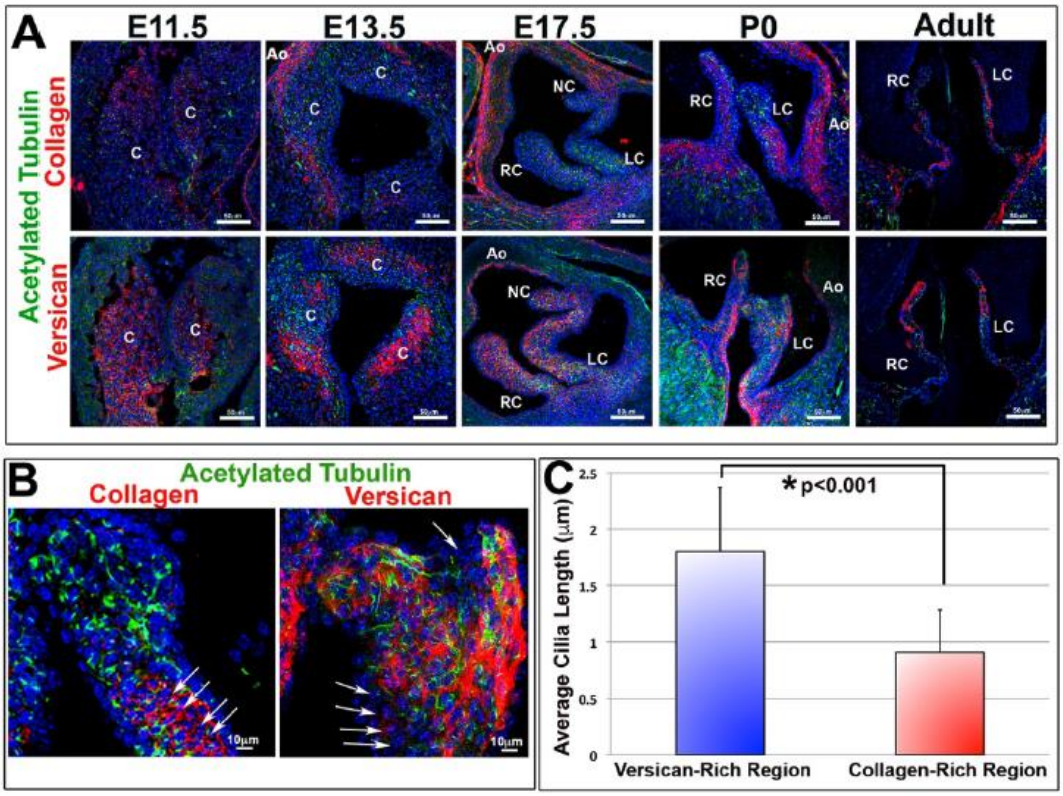

Figure 2.2 Primary Cilia Expression Co-Localized with Proteoglycans in Valve Development. (A) Immunohistochemistry for the ciliary axoneme (green), collagen (red, top) versican (red, bottom), and nuclei (blue) show expression of cilia throughout development. Cilia appear to be expressed highly in areas rich in proteoglycans and less in areas high in collagen. C= conal cushions, RC= right coronary, LC=left coronary, NC= non-coronary, Ao= aorta. (B) High magnification images of axonemes (green) and collagen/versican (red). Arrows depict collagen rich regions expressing shortened cilia. (C) Quantification of cilia length in both versican and collagen rich regions shows decreased average cilia length in collagen rich regions when compared with versican rich regions, $p<0.001$ t-test (Image by Katelynn Toomer).

A New Cilia Gene Found Linked to MVP

By uncovering the expression of primary cilia and its regions of specificity on the mitral valve during development, we took a separate approach on investigating a commonality for the disease. To start, a GWAS was performed across a wide range of the human genome in an effort to identify genetic risk factors within the population. This study was followed by a sequential linkage analysis that was conducted on a large non-syndromic family with MVP to find a commonality for this disease. Through this study the linkage analysis identified a specific region on chromosome 13 and among the different genes that were found, a cilia gene called *DZIP1* was identified (Figure 2.3).

Protein Expression of Dzip1

DZIP1 is classified as a DAZ Interacting Zinc Finger Protein and has previously been implicated in a disease called Acrodermatitis Enteropathica (AE). As mutations in this gene has been shown to cause the inability to absorb zinc from the intestine. This can result in skin inflammation on various parts of the body, because there is a significant lack of zinc. Knowing this characteristic, we also see DZIP1 in various signaling pathways, Hh and signaling through GPCR and most recently we see DZIP1 required for the formation of cilia. Through our vast studies within the lab we were able to identify cilia as an organelle that played a major role in the development of the mitral valves. We discovered DZIP1 as a key player in our current research by evaluating several different families with non-syndromic MVP through GWAS (1412 MVP and 2439 controls).

Through immunohistochemistry application the expression of Dzip1 is seen on the mitral valve expression patterns of Dzip1 have been seen to co-localize to the base of the ciliary axoneme (Figure 2.4). Furthermore, we investigated whether or not the phenotype

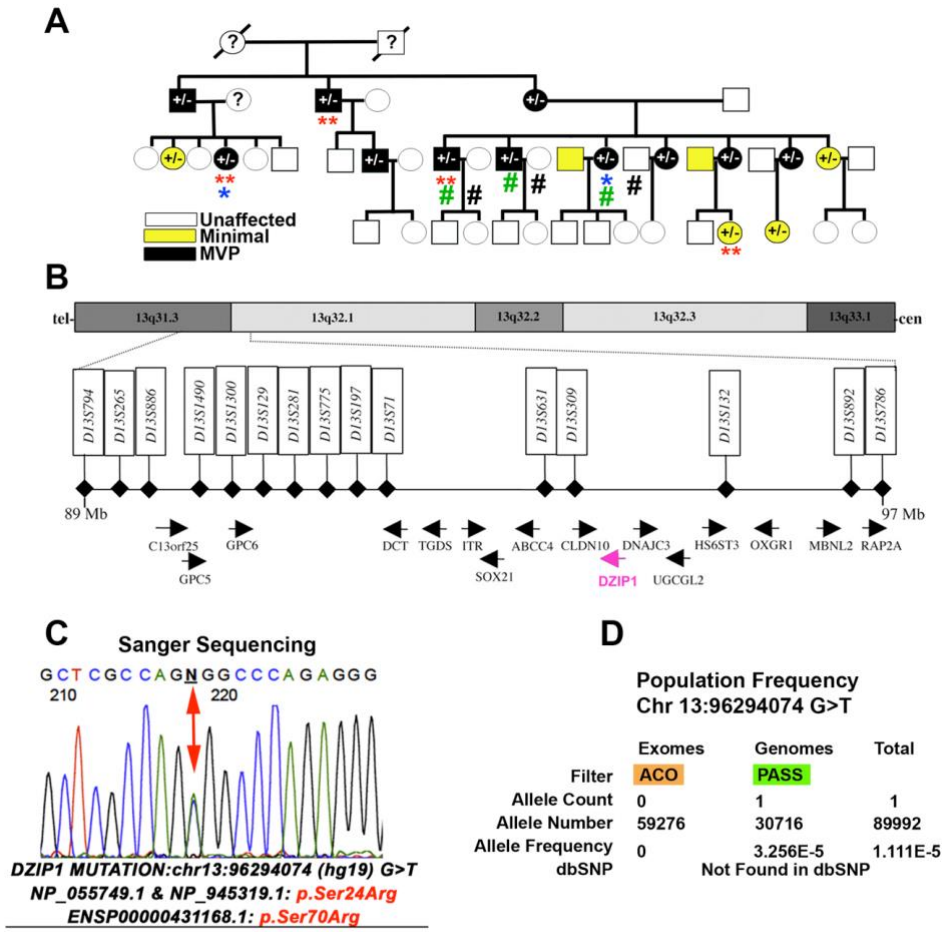

Figure 2.3 Identification of *DZIP1* as an MVP Gene. **(A)** Multigenerational family with inherited, autosomal-dominant, non-syndromic MVP. Black circles and squares are affected individuals, green circles and squares are individuals who exhibit minimal MVP, white circles and squares are unaffected. Circles=female, squares=male. ID designations for family members are denoted under the circles or squares. Proband is identified with the black arrow. **(B)** Human transcript and marker maps of the linkage interval on chromosome 13. Candidate region is within 13q31.3-32.1, and all *RefSeq* genes and their orientations are shown within the 8.2-Mb interval. *DZIP1*, the only cilia gene within the locus, is highlighted in pink. **(C)** Sanger sequencing identified a single missense mutation within exon 5 of *DZIP1* resulting in a serine to arginine change. The mutation segregates with the affected patients and is designated by +/- in the pedigree. **(D)** Population frequency showing the rarity of the identified DZIP1 variant in the population (Image by Dr. Russell Norris, Science Translational Medicine, Accepted 2019).

that is exhibited in our MVP patients could be seen in a mouse model. Therefore, a *Dzip1*$^{S14R/+}$ knock-in mouse was created using CRISPR (Clustered Regularly Interspaced Short Palindromic Repeat) technology by geneticists at the Medical University of South Carolina. They were able to successfully knock-in the exact DZIP1 mutation that was also exhibited in our MVP patients (Figure 2.5) and through histological applications it was determined that our *Dzip1*$^{S14R/+}$ knock-in mice revealed MVP phenotypes as well like myxomatous degeneration (Figure 2.6). In order to gain more insight on how mutations in DZIP1 cause MVP, a two-hybrid screening was performed. In the results of the two-hybrid screening we found a pre-mRNA processing protein, called Prpf8, to interact with our wild type DZIP1 plasmid component and not our mutant DZIP1 component. Prpf8 is considered the heart of the spliceosome as it is a main factor in regulating mRNA splicing (Grainger & Beggs, 2005). Protein expression of both Prpf8 and Dzip1 were also measured in adult tail fibroblasts taken from mouse models: wild type (*Dzip1*$^{+/+}$) and mutant (*Dzip1*$^{S14R/+}$ and *Dzip1*$^{S14R/S14R}$), where we saw a decrease in expression in the mutant protein compared to wild type (Figure 2.7). This is the first indicator that there is a difference in gene expression possibly due to the point mutation in *Dzip1*.Therefore, we concluded that our data from familial and genome wide association studies have indicated that DZIP1 and an interacting protein, Prpf8 may provide additional clues for how ciliogenesis can be controlled.

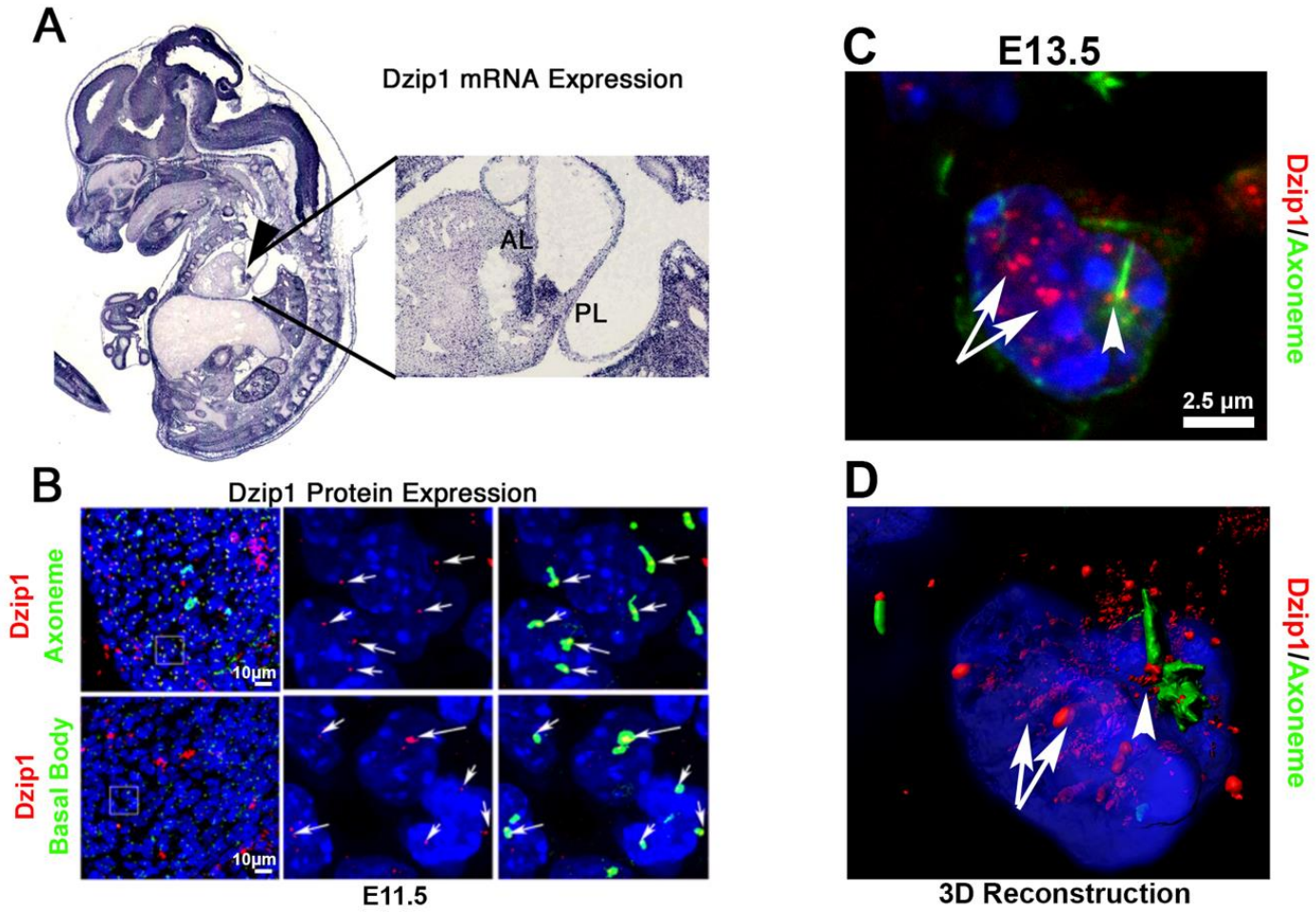

Figure 2.4 Dzip1 is Expressed at the Base of Primary Cilia in the Murine Mitral Valve. (A) Section of the mitral valve in situ at E14.5 shows robust Dzip1 mRNA expression in the anterior and posterior mitral leaflets (AL, PL, respectively). **(B)** IHC for Dzip1 (red) and axonemes (green) or basal bodies (green) showing expression of Dzip1 at the basal body in E10.5 AV cushion mesenchyme. **(C)** Max projection image from high-resolution confocal microscopy of an E13.5 AV cushion mesenchymal cell showing Dzip1 (red) localized to the base of the ciliary axoneme (arrowhead) and the nucleus (arrows). **(D)** 3D reconstruction of the image in panel C created from the confocal z-stack file (Image by Diana Fulmer, Norris Lab).

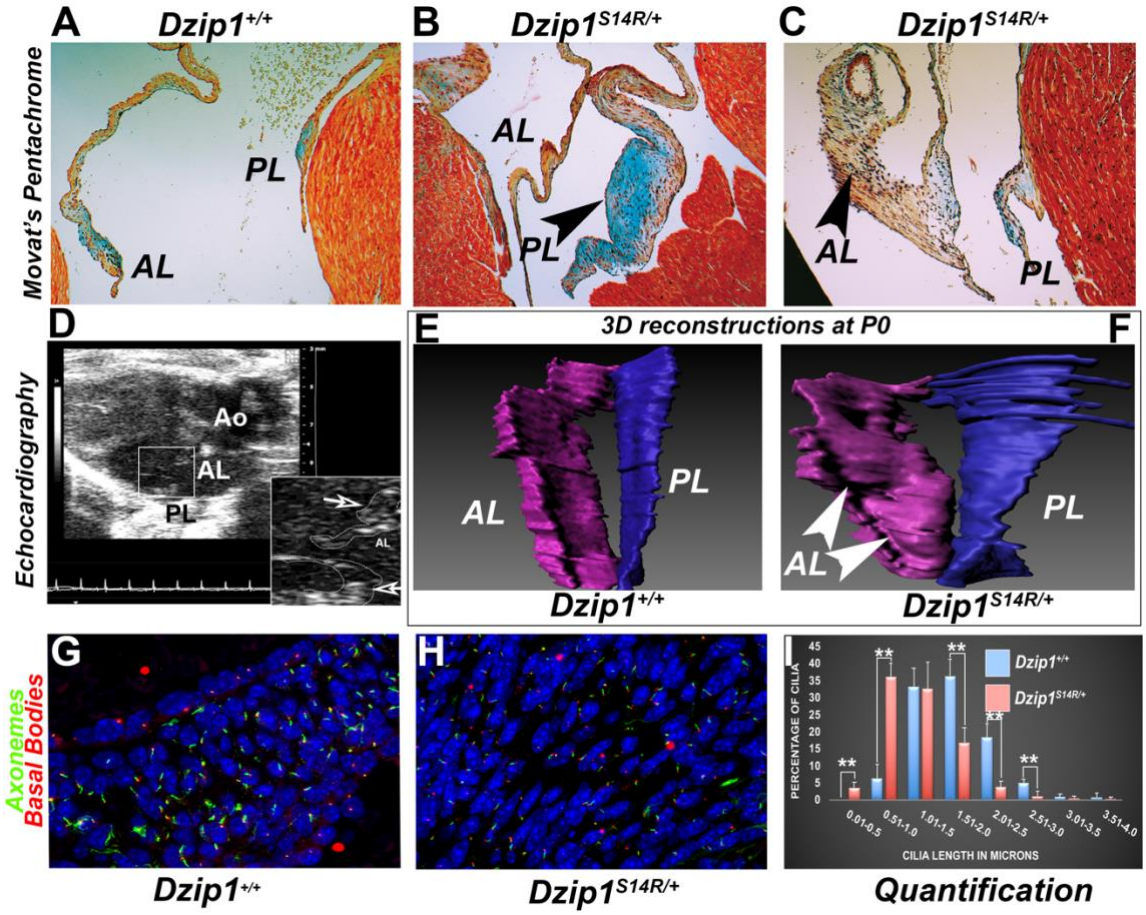

Figure 2.5 Developmental Basis for Non-syndromic MVP. (A-C) Movats Pentachrome staining shows valve enlargement, elongation, and myxomatous degeneration in the *Dzip1*$^{S14R/+}$ mitral anterior and posterior leaflets (Al, PL) compared to control (*Dzip1*$^{+/+}$). n=4/genotype. **(D)** Echocardiography of adult (6-month-old) *Dzip1*$^{S14R/+}$ mice shows thickened and elongated anterior and posterior leaflets (AL, PL) that prolapse into the left atrium. n=4/genotype. (**E, F**) 3D reconstructions show bulging and excess tissue in the anterior leaflet (arrowheads) and an elongated posterior leaflet in *Dzip1*$^{S14R/+}$mice compare to controls (*Dzip1*$^{+/+}$). (**G-I**) IHC shows shortened and loss of axonemes (green) in the *Dzip1*$^{S14R/+}$ mitral leaflets, ***p*<.*01*. Red-basal bodies (gamma tubulin), Blue- nuclei (Hoescht). For each of these studies, n=5/genotype (Image by Diana Fulmer, Norris Lab).

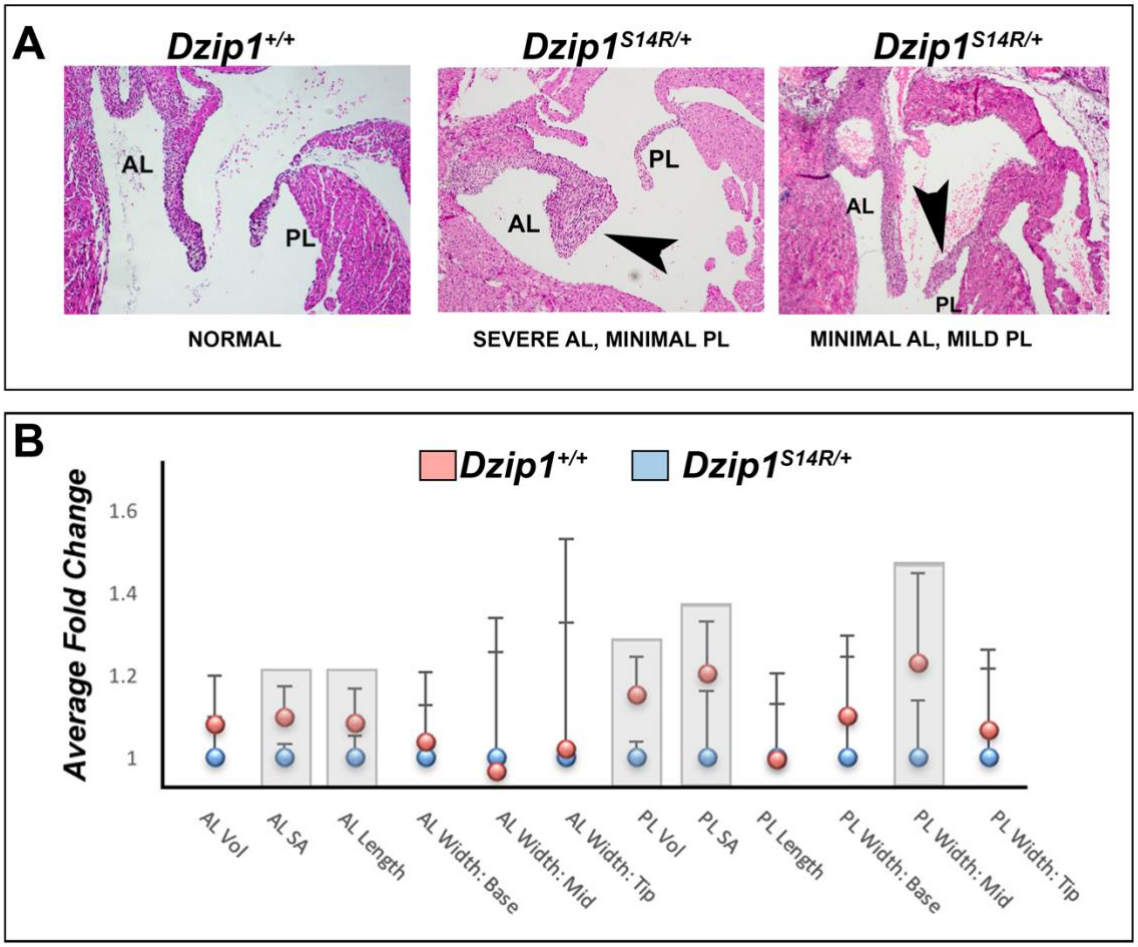

Figure 2.6 *Dzip1*$^{S14R/+}$ Point Mutation Results in a Congenital Dysmorphic Mitral Valve Phenotype. (A) H&E staining of mitral valves from control (*Dzip1*$^{+/+}$) and Dzip1 point mutation knock-in (*Dzip1*$^{S14R/+}$) mice shows dysmorphic anterior and posterior leaflets at P0. Arrowheads point to valve leaflets of irregular shape in the knock-in model (*Dzip1*$^{S14R/+}$) compared to controls (*Dzip1*$^{+/+}$). **(B)** Quantification of valve 3D reconstructions of wild type and *Dzip1*$^{S14R/+}$ point mutation mitral leaflets. n=5 animals/genotype analyzed, and error bars represent standard error of mean. * p-value <0.05. AL, PL=anterior and posterior leaflets, respectively (Image by Diana Fulmer, Norris Lab).

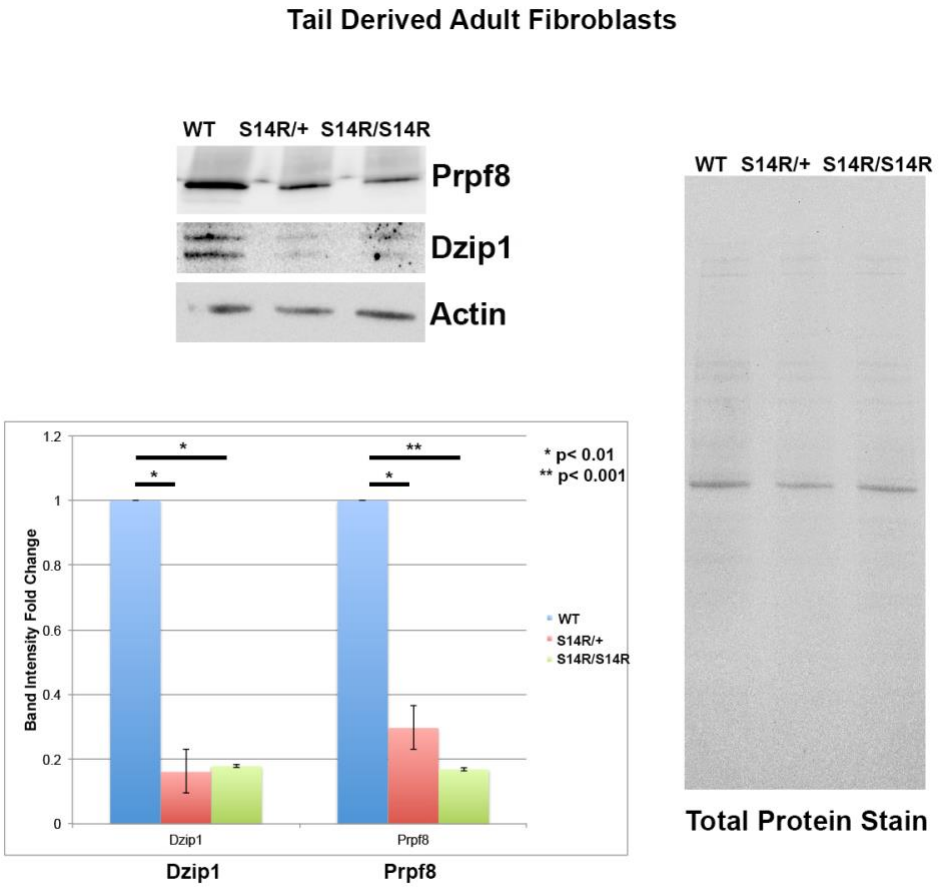

Figure 2.7 Protein Expression of Prpf8 and Dzip1 in Adult Tail Fibroblasts. Adult tail fibroblasts were isolated from *Dzip1*$^{+/+}$, *Dzip1*$^{S14R/+}$ and *Dzip1*$^{S14R/S14R}$ animal models and had less Dzip1 protein expression than the control. Protein expression of *Dzip1*$^{S14R/+}$ and *Dzip1*$^{S14R/S14R}$ quantified at molecular weights: 105 kDa and 99 kDa had a significant decrease (noted *= p value is <0.05 and **= p-value is <0.0005) in Dzip1 protein expression (Image by Diana Fulmer, Norris Lab).

Two- Hybrid Screening

The Two- Hybrid Screening was designed to establish direct protein-protein interactions by a simple bait-prey concept that examined the physical interactions of the protein(s) in question. The basis behind this technology can uncover various proteins as well as DNA interactions that can lead to a network of integrated components. In the relation to our studies with MVP and our discovery of DZIP1, a yeast two-hybrid (Y2H) was performed to discover the binding partners of Dzip1. Traditionally, the Y2H, looks at protein interactions through reporter genes that are activated once one is detected in the bait and prey system. These reporter genes enable a distinct color reaction and the cDNA-library screen searches for pairwise interactions between defined proteins of interest (bait) and their interaction partners (preys) present in cDNA libraries or sub-pools of libraries. Here, preys are not separated on an array but pooled and libraries may contain cDNA fragments in addition to full length ORFs, thus largely covering a transcriptome and reducing the rate of false negatives (Bruckner, Polge, Lentze, Auerbach, & Schlattner, 2009).

Given this technique, we decided to look at both wild type DZIP1 plasmid and mutant DZIP1 plasmid to see what interactions we could discover. Through this study we found numerous proteins that interacted with the wild type DIZP1 but uniquely enough there was only one protein that did not interact with our mutant DZIP1 plasmid, Prpf8. Being that Prpf8 was our only protein found to not interact with the mutant DZIP1 plasmid, we hypothesized that:

The Dzip1 regulation of ciliogenesis through a Prpf8 mRNA splicing mechanism is broadly involved in MVP disease.

At the heart of the spliceosome

Prpf8 is classified as a splicing factor and mutations associated with Prpf8 result in a disease called retinitis pigmentosa. The design behind the pre-mRNA splicing mechanism is extremely intricate, as each step is important in forming a mature mRNA strand, which is through the spliceosome which removes introns. Pre-mRNA splicing is made up of two *trans*-esterfication reactions within the spliceosome complex. Prpf8 is the central component of the spliceosome and is considered the essential factor of this unique complex (Figure 2.8). The components of the spliceosome are made up of small nuclear RNA-protein complexes: U1, U2, U4, U5 and U6. Prpf8 is a component of the U5 and the tri-snRNP formed with U5+U4/U6. The snRNPs are encountered by various RNA-dependent NTPases/RNA unwindases that catalyze each *trans*-esterification reaction, progressing the spliceosome to perform its job. Although, Prpf8 has been established as a splicing factor, its classification took a series of experiments to confirm.

In 1967, Lee Hartwell and coworkers performed a genetic screen to isolate temperature-sensitive (ts) mutations in *Saccharomyces cerevisiae* (Hartwell, McLaughlin, & Warner, 1970). They identified 10 complementation groups, *rna2-rna11,* of mutations that caused accumulation of RNA following a shift from the permissive (23°C) to the restrictive (36°C) temperature. Many of these *RNA* genes were later renamed *PRP* genes, to indicate their involvement with pre-mRNA processing (Vijayraghavan, Company, & Abelson, 1989). These results identified the *RNA8/PRP8* gene product as an essential mRNA splicing factor that was involved early in the splicing process.

Finally, the discovery of Prpf8 was crucial in fully understanding the pre-mRNA splicing process, making it primarily seen within the nucleus on heart tissue once stained. A

previous study focused on Prpf8 and its association with primary cilia and found the Prpf8 localized to the base of the basal body. This insight was very informational as we were beginning to unfold both Dzip1 and Prpf8's role in primary cilia (Wheway et al., 2015).

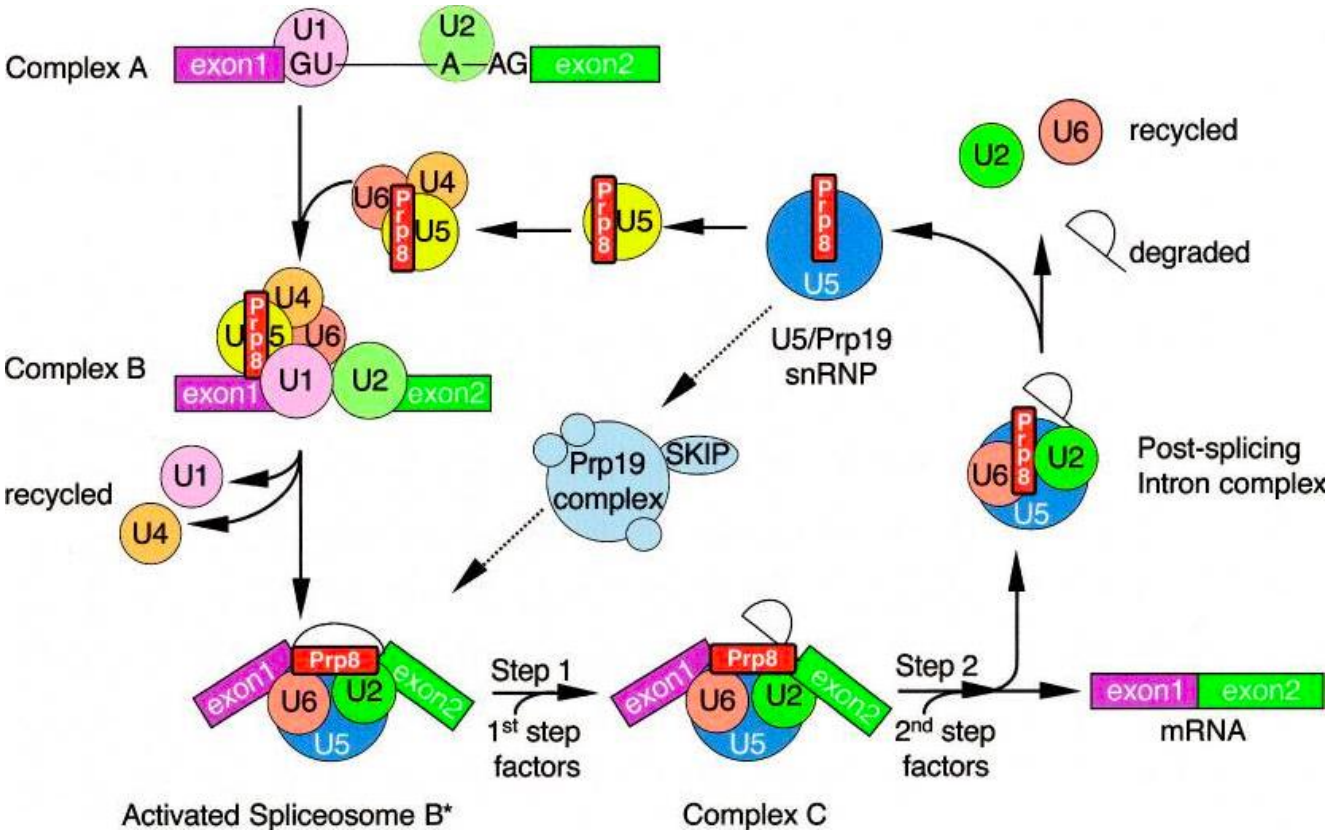

Figure 2.8 The Cycle of the Spliceosome. Schematic diagram showing the assembly and recycling of spliceosome components, with respect to Prpf8. Prpf8 has been found in two different U5 complexes: the U5 snRNP (small, yellow) and the larger U5/Prp19 snRNP (large, blue) (Makarov et al., 2002)©

Protein Expression of Dzip1 and Prpf8

The expression of Dzip1 was analyzed through immunohistochemistry stains, co-staining with cilia biomarkers. Dzip1 can be seen co-localized to the base of the ciliary axoneme, throughout valve development. (Figure 2.9). This coincides with the role of Dzip1 as it is required for ciliogenesis. Being that Prpf8 is a splicing factor, its expression is primarily within the nucleus, seen on immunohistochemical stains. Although, a previous study has also found that Prpf8 is expressed at the base of the basal body of primary cilia.

Preliminary data was also performed by western blot analysis to confirm that there is more of presence of Dzip1 and Prpf8 in wild type compared to mutant mouse model. This was evaluated by collecting protein from mouse models (*Dzip1*$^{+/+}$ and *Dzip1*$^{S14R/+}$) and probing for Dzip1 and Prpf8 with their respective antibodies (Figure 1.7). By analyzing the results of the Two-Hybrid Screening, we were able to start the journey of uncovering the connection between the two proteins, Dzip1 and Prpf8. Our first step was to confirm that both, Prpf8 and Dzip1 were co-expressed and co-localized together on the mitral valves. To verify this further immunohistochemical stains were performed co-staining for both proteins on *Dzip1*$^{+/+}$ heart tissue. Stains show that the proteins are in fact co-expressed and co-localized with one another on the mitral valves.

Validation of Two-Hybrid Screening

Given the information provided from the Two-Hybrid Screening we looked to reproduce those results. Therefore, we performed a co-immunoprecipitation, where we collected protein from adult tail fibroblasts from our wild type and diseased knock-in

mouse model. We simply immunoprecipitated the protein with Prpf8 IgG and probed for Dzip1.

Through this application we were able to directly verify that the Dzip1 mutation impairs interaction with Prpf8 as we experienced a loss of Dzip1 (Figure 2.10).

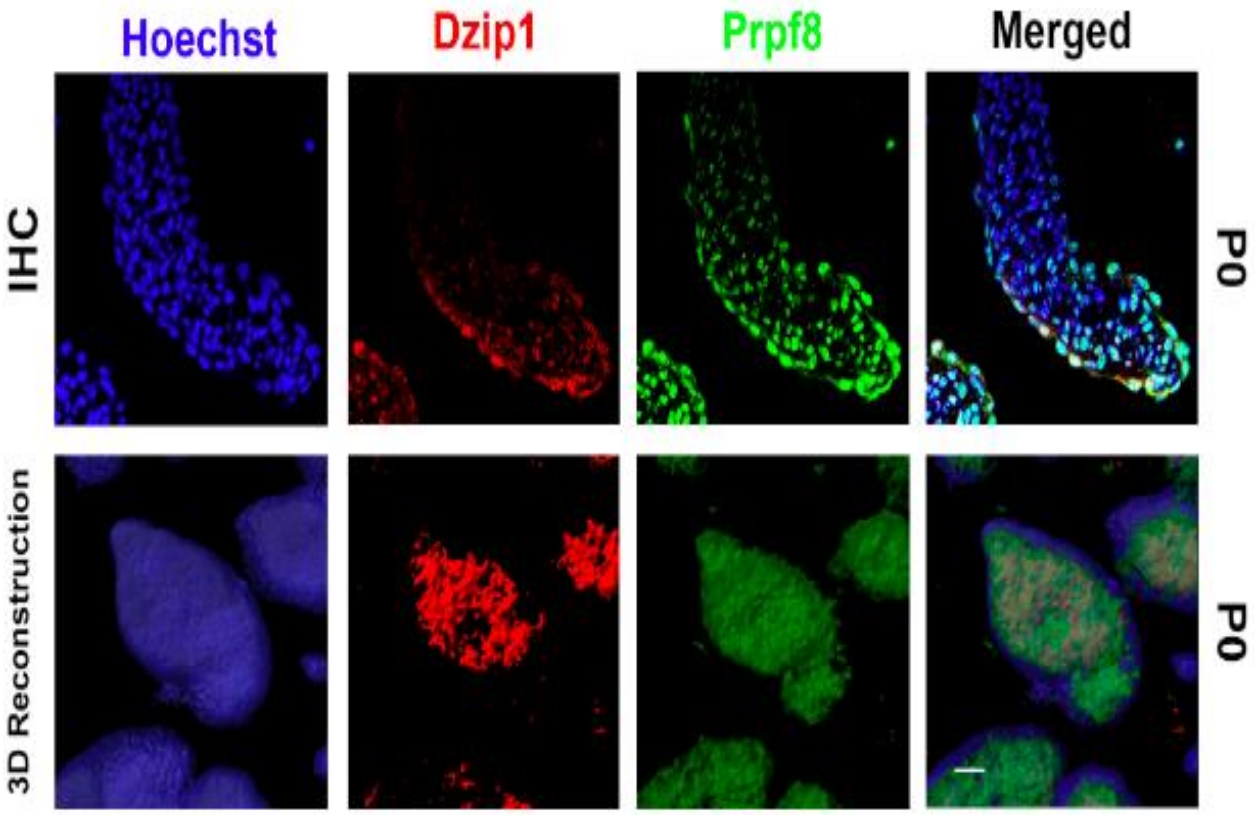

Figure 2.9 Prpf8 and Dzip1 Expression on the Valve. (A) Immunohistochemistry on wild type mouse heart tissue shows Dzip1 (red), Prpf8 (green) and nuclei (blue) being expressed on the posterior leaflet at postnatal age P0. **(Bottom panel)** is a 3D reconstruction image completed with Imaris software to show at a greater magnification (63X5) to show co-localization with Prpf8 (green) and Dxip1 (red).

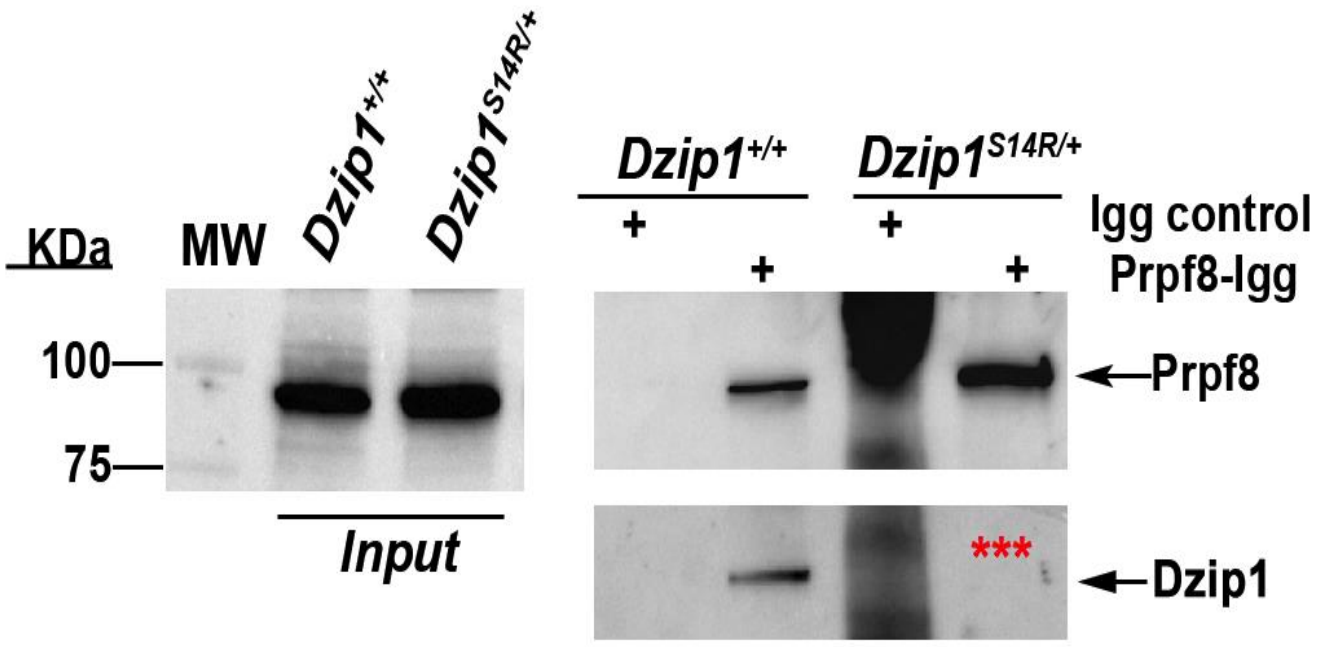

Figure 2.10 Dzip1 Mutation Alters Prpf8 Interaction. Co-IP showing that the Dzip1^{S14R} mutation impairs interactions with the PRPF8 splicing factor. Endogenous proteins were immunoprecipitated with Prpf8 IgG and probed with Dzip1. Prpf8 binding is greatly reduced (asterisk) in the mutant. Prpf8 was probed on the same blot to ensure comparable amounts of protein was immunoprecipitated. Input lanes showing total Dzip1 protein expression is indicated on the left.

Discussion

Although the genetics behind MVP are still developing, the beginning stages of fully understanding which genes cause this disease are examined through these various studies. The mechanism by which *Dzip1*$^{S14R/+}$ causes MVP is still not understood but as we take a closer look at Dzip1 and Prpf8 we begin to form a broad hypothesis that the mechanism by which Dzip1 mutations result in MVP is directly related to mRNA splicing, via splicing factor Prpf8.

These studies illustrate the interaction between Dzip1 and Prpf8 is present as is a loss of protein expression in mutant mouse model. The mutation impairs interaction between Prpf8 and Dzip1 and this gives us a broad idea of how the two are interacting and that the mutation is significantly affecting that interaction.

Further experiments are needed to firmly understand at which point in time the two protein interact and by which mutations in Dzip1 cause a disruption of Prpf8 not performing its main role properly.

In order to further investigate this, plausible pathways in which the two are interacting needs to be determined. For instance, known signaling pathways in relation to primary cilia are: Hh, Wnt, Notch, and TGFb to name a few. In addition, truncation experiments can be completed to narrow down even further a closer timepoint.

CHAPTER 3: CILIARY TARGETS REVEALED

Introduction

There has been much debate on whether primary cilia play a role in early age development. Before there was any evidence on these organelles, many believed that they simply held no significant function. However, through several studies we know this notion to be false. We have learned that not only are primary cilia expressed on the mitral valves (heart) during early development but they are expressed on the kidney, retinal, and neurological cells. There has been genetic evidence that have directly associated mutations in cilia to a plethora of diseases that afflict the liver, heart and brain. This is an example of a ciliopathy, which is when a genetic mutation encoding defective proteins results in the abnormal function or formation of primary cilia (Beales et al., 2007). The term ciliopathy was first coined when Ansley et. al discovered genetic mutations in *BBS8,* which resulted in the phenotype of Bardet-Biedl syndrome (BSS) (Ansley et al., 2003). This finding paved the way for further investigations on how organelles that were thought to be nonsignificant affect normal function in development.

To date, approximately 1,000 polypeptides have been linked within the ciliary proteome (Gherman, Davis, & Katsanis, 2006). Specifically, mutations in *IFT80,* encodes an intraflagellar transport protein in a subset of patients with Jeune asphyxiating thoracic dystrophy (JATD). It has been found that patients with JATD exhibited typical ciliopathy features like retinal degeneration, renal disease and skeletal dysplasia (Beales et al., 2007). This has led to many studies that centered around exploring the signaling mechanisms and the proteins involved in the building of primary cilia, which is known as ciliogenesis. Many researchers have explored the pathways of Wnt and Hedgehog signaling as well as the proteins involved in these pathways. Specifically, it has been

found that through several genetic screens that there is a connection between mammalian Hh signaling and intraflagellar transport (IFT). For example, Ift88, Gli family members and Smoothened (Smo). Recent studies within our lab have identified the direct association with Hh signaling and primary cilia during mitral valve development.

Results

Hedgehog Signaling

Hedgehog Signaling has become one of the most well-studied signaling pathways that has been directly associated to primary cilia. This pathway has been essential for development in many organs. Evidence has shown that many components involved in Hedgehog signaling have co-localized to base of primary cilia (Figure 3.1). In this pathway there are receptors, Patched (Ptch1) and Smo that travel up and down the axoneme of the cilia. They do this as a response to the hedgehog ligands: sonic (Shh), Indian (Ihh) and desert (Dhh). Patched is considered a negative regulator of this pathway because in the absence of ligand Ptch1 inhibits the activation of Smo. While, in the presence of Hh ligand Ptch1 removes the inhibition of Smo and allowing it to move up the ciliary axoneme. As Smo enters the ciliary axoneme it interacts with Sufu, which in turn allows the processing of Gli family members: Gli1, Gli2 and Gli3). In regard to Gli transcription factors they can be either activators or repressors. If there is absence of Hh ligand then the Gli transcription factors are restricted to their repressor forms. As we begin to look at other components involved in ciliogenesis, we discover the important role that IFT proteins play in Hh signaling. Knowing this our lab examined the loss of Ift88, which is a centrosomal protein required for ciliogenesis. Compared to the wild type

there is an increase in the enlargement of the ECM (Figure 3.2) in our *Ift88$^{f/f}$ NfatC Cre+* mouse model.

As mentioned earlier Gli transcription factors can either be in a repressed (GliR) or active state (GliA). IFT proteins are required for the production of GliA and GliR and consequently the disruption of these proteins disrupts Hh signaling (Haycraft et al., 2007). Each transcription factor of Gli plays an important role in development as they are directly involved in Hh signaling. To summarize the activation of Gli1 activates that Hh pathway through Gli2 and Gli3 activation. Gli2 is responsible for regulating fibrotic signals and Gli3 is essential for basal suppression of the Hh pathway. All of which directly and indirectly affect the progression of ECM genes downstream in Hh. This notably is another important step in valve development.

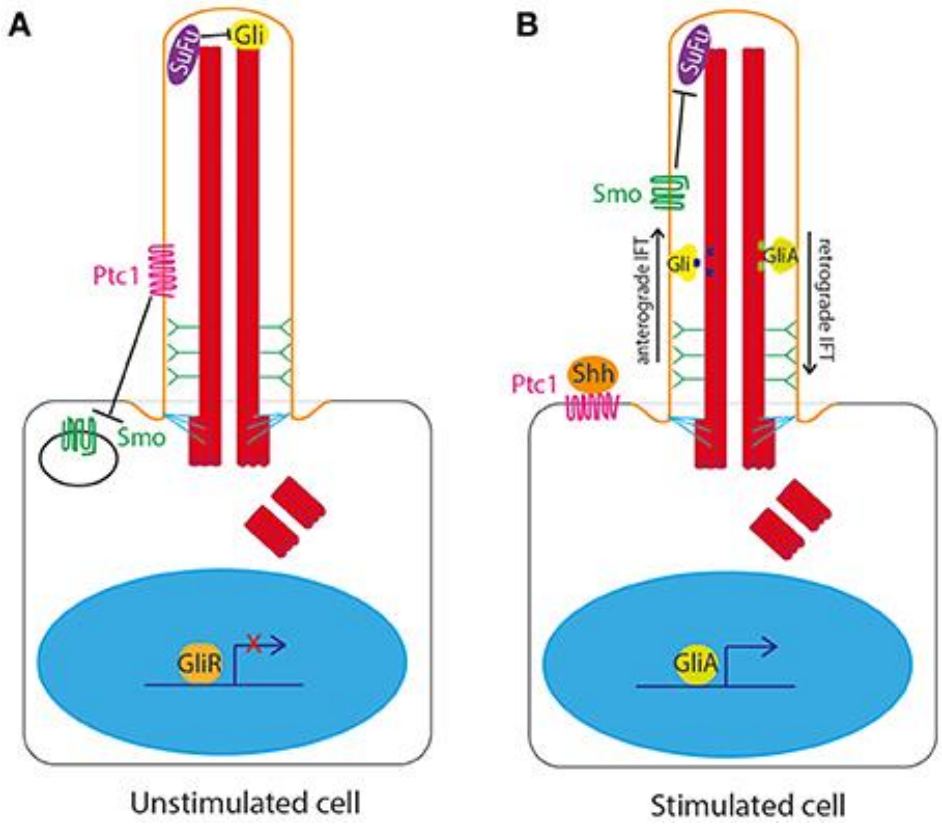

Figure 3.1 Hedgehog Signaling through Primary Cilia. Hedgehog signaling at the primary cilium in vertebrates. **(A)** In the unstimulated state, Ptc1 sits in the cilium membrane and represses and excludes Smoothened (Smo) from the cilium. Gli transcription factors are sequestered and suppressed by Suppressor of Fused (SuFu) at the tip of the primary cilium. **(B)** In the stimulated state, upon binding of Shh to Ptc1, the repression of Smo by Ptc1 is relieved, allowing Smo to enter the cilium and Ptc1 to leave the cilium. This then allows Smo to repress SuFu, relieving repression of Gli at the tip of the cilium. Gli is thus freed to be post-translationally modified to form Gli activator form (GliA), which is transported out of the cilium to the nucleus to activate expression of downstream target genes (Wheway, Nazlamova, & Hancock, 2018). ©

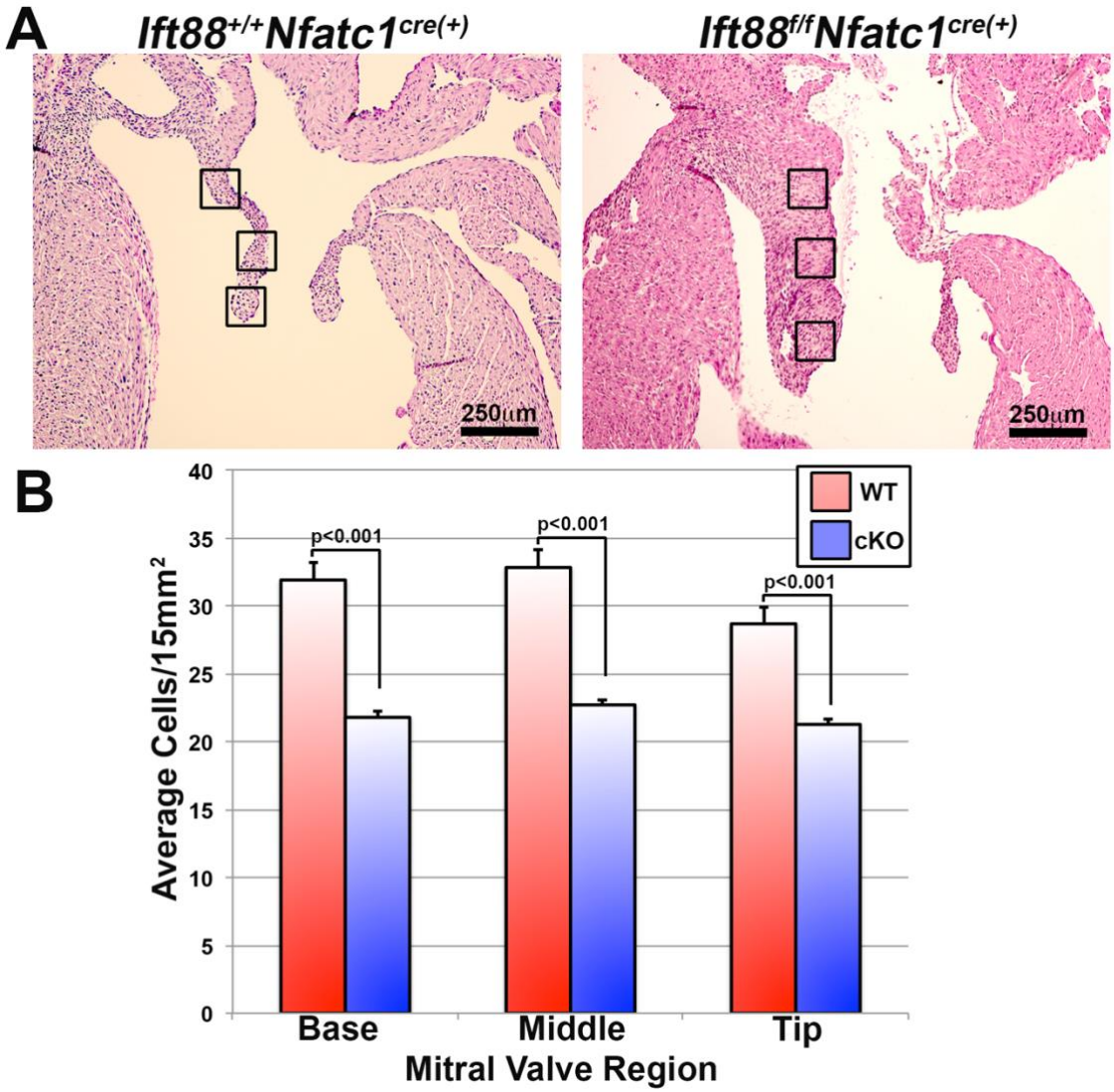

Figure 3.2 Loss of Ift88 Results in Myxomatous Degeneration. (A) H&E staining and 3D reconstructions show that loss of *Ift88* results in valve enlargement in both anterior and posterior leaflets (black arrowheads). **(B)** Quantification of valve 3D reconstructions of control (*NfatC1*$^{Cre(+);}$*Ift88*$^{+/+}$) and *Ift88* conditional knockout (*NfatC1*$^{Cre(+)}$*;Ift88*$^{f/f}$) mitral leaflets. **p-value*<*.001*. n=6 for conditional knockout and n=4 for control (Image by Katelynn Toomer, Norris Lab).

Differences in Gene Expression

A cell's function is dependent on its complex transcriptional material. Many researchers have turned to RNASeq, a technique that provides fundamental information from within the cell. Furthermore, this application can examine the expression levels of genes and deliver knowledge on genes that have yet to be discovered. It has also been demonstrated that splicing variants and single nucleotide polymorphisms (Sultana & Wang, 2008). can be detected through sequencing the transcriptome, opening up the opportunity to interrogate allele-specific expression and RNA editing. Knowing the impact that IFT proteins have on the building of primary cilia, we designed mouse models: NfatC1$^{Cre(+)}$; Ift88$^{f/f}$ and NfatC1$^{Cre(-)}$, Ift88$^{+/+}$ (Figure 3.3). In our NfatC1$^{Cre(+)}$; Ift88$^{f/f}$ model we see almost a complete ablation of primary cilia, where any remaining cilia is severely shortened compared to our NfatC1$^{Cre(-)}$, Ift88$^{+/+}$. Therefore, to study the differences in gene expression we conducted a RNASeq analysis where we dissected mitral valve leaflets from our Dzip1 knockin and wild type mouse models and isolated RNA (Figure 3.4).

This study paved the way for us to perform the same study on our knockin mouse models, *Dzip1*$^{S14R/+}$ *and Dzip1*$^{+/+}$. Through examining these two models we found a significant difference in gene expression in subsequently the protein Ift88. As stated earlier Ift88 is a centrosomal protein and is required for ciliogenesis. This discovery made Ift88 a plausible ciliary target for Prpf8 as we believe that this splicing factor would not be able to fulfill its job correctly in the presence of the Dzip1 mutation. Overall, the differences in gene expression was the first indicator that there is possibly another factor at play (Draghici et al., 2007)

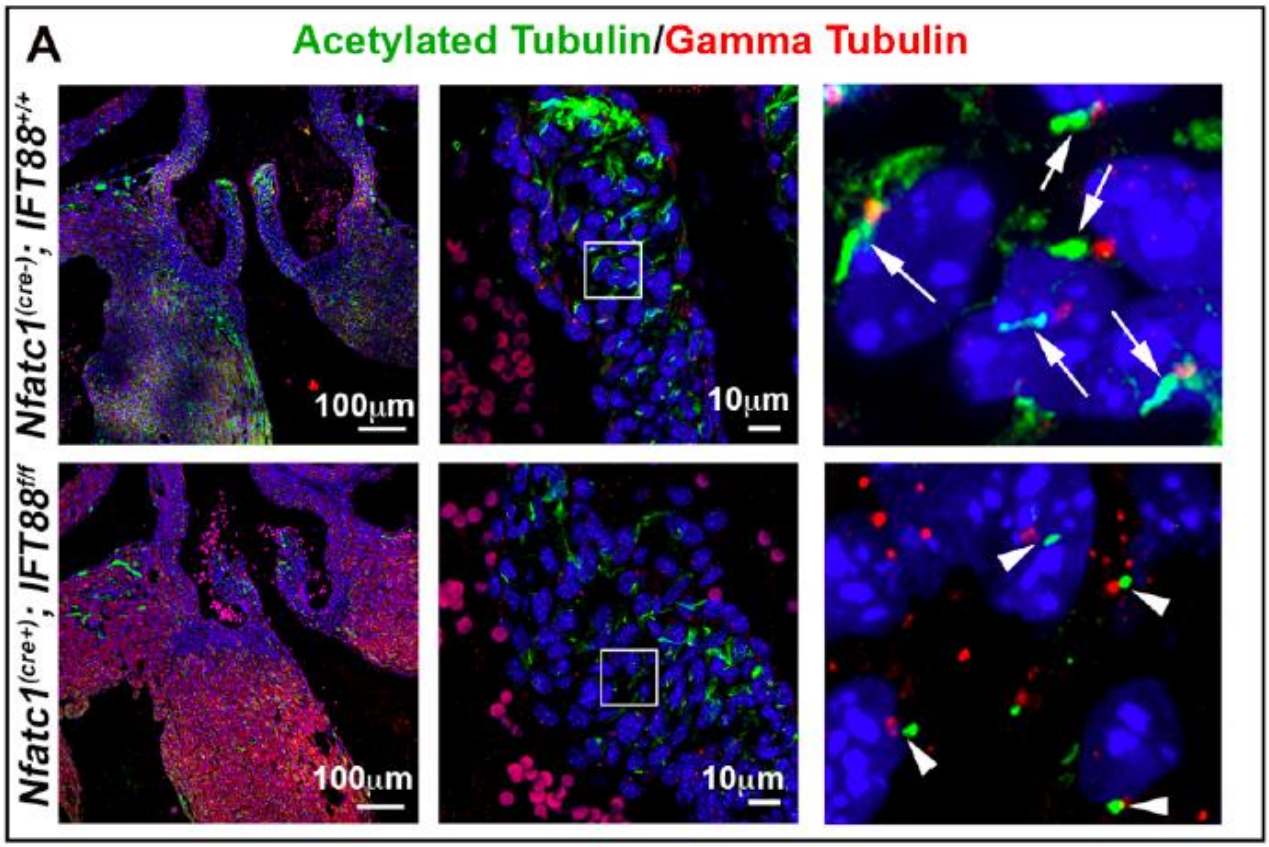

Figure 3.3 Loss of Cilia in Ift88$^{f/f}$ Nfatc1 Mice. IHC showing loss of cilia expression in conditional knockout animals. Axonemes in green and basal bodies in red. Arrows pointing to cilia expression; arrow heads pointing to loss or shortened cilia (Image by Katelynn Toomer, Norris Lab).

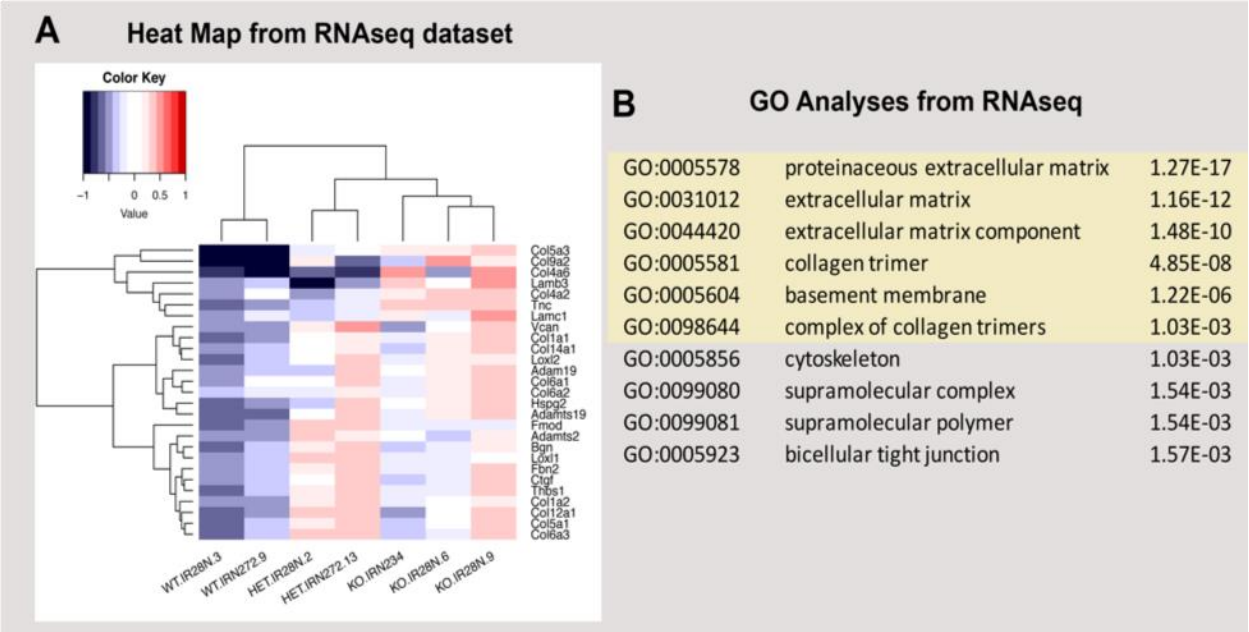

Figure 3.4 RNAseq Analyses Correlate Loss of Cilia with ECM Gene Activation. (A) Heat map of RNAseq data from the anterior leaflets of *Ift88* conditional knockout (*NfatC1*$^{Cre(+)}$*;Ift88*$^{f/f}$) and control (*NfatC1*$^{Cre(+)}$*;Ift88*$^{+/+}$) P0 mitral valves showed large increases in the expression of extra cellular matrix gene transcripts. **(B)** GO analyses of an additional RNAseq dataset also revealed an upregulation of ECM gene pathways in *Dzip1*$^{S14R/+}$ hearts compared to controls at E13.5, supporting the previous findings at a timepoint before the onset of disease morphology (Image by Dr. Russell Norris).

Alternative Splicing

RNASeq intricately evaluates gene expression within the cell. Yet, DEXSeq tackles the regulation of these processes requires sensitive and specific detection of differential isoform abundance in comparisons between conditions, cell types, or tissues. Therefore, we use DEXSeq to test for differential exon usage from the RNASeq data obtained previously. Specifically, the DEXSeq uses generalized linear models and offers reliable control of false discoveries by taking biological variation into account. This method also enables the study of regulation and function of alternative exon usage on a genome-wide scale. (Anders et.al 2012). Transcript count data from the analysis of the samples were sorted according to their adjusted p-value or q-value, which is the smallest false discovery rate (FDR) at which a transcript is called significant. Resulting in a list of significant genes that were alternatively spliced between the mouse models: *Dzip1*$^{S14R/+}$ *and Dzip1*$^{+/+}$. Furthering the investigation behind uncovering the possible role splicing played between the two models. In order to ensure that the results we received had a basis we completed a series of western blots to examine a difference in splicing in these significant proteins. Ultimately, this would give us knowledge on which proteins are being affected by this mutation in *DZIP1*.

Table 3.1 Alternative Splicing Detected. The list of genes that had differential exon usage in *Dzip1*$^{+/+}$ compared to *Dzip1*$^{S14R/+}$ mouse valve leaflets. The exon (s) that undergoes alternative splicing is identified along with its p-value.

Table 3.1 Genes with alternative splicing in mutant Dzip1 valve leaflets compared to wild type Dzip1.

Gene Name	Exon Number	p-value
Rab11a	E1	9.02e-08
Sept7	E36	1.58e-07
Tuba1a	E2	7.45e-07
Tubgcp3	E2	0.00030098
Smo	E14	0.00045523
Glis2	E7	0.00067927
Ift88	E19-24	<1X10e-09

Ciliary Targets Revealed

The DEXSeq was the next step in pinpointing the differences in splicing in the presence of the mutation found in *Dzip1*$^{S14R/+}$. As it has been previously mentioned Prpf8 is a central component of the spliceosome, making its role critical in pre-mRNA splicing. Knowing this knowledge, we closely examined the genes that were being alternatively spliced. A few of the genes found had been implicated in the process of ciliogenesis, for example, Ift88 and Smo, because of this factor it fueled the notion that in the presence of the point mutation Prpf8 is unable to perform its job correctly, subsequently disrupting the formation of primary cilia. To investigate this further a western Blot analysis was used to identify alternative splicing. Protein was collected from mouse embryonic fibroblasts, both wild type and mutant to evaluate a change in expression.

Furthermore, this expression was seen in the following targets, probed with their respective antibodies: Tubgcp3 (Tubulin Gamma Complex Associated Protein 3), Ift88, and Glis2 (GLI Zinc Finger Protein 2). While these are only a few of the proteins identified in the DEXSeq, these proteins showed a significant change, quantified through western blot analysis (Figure 3.5). Although there was no significant data obtained through western blot analysis that supports Smo being alternatively spliced, other genes like Tubgcp3 and Glis2 prove otherwise. All of these genes have been previously associated with the building of primary cilia. For instance, TUBGCP3 job consists mainly of gamma-tubulin binding. Tubgcp3 is a cilia- associated protein and mutations of *TUBGCP3* can lead to cardiomyopathy, Dilated, 1P (Spudich, 2014) (Lu et al., 2015). Recent studies show that the loss of *GLIS2* leads to diseases like progressive kidney atrophy, interstitial inflammatory infiltration, and fibrosis (Attanasio et al., 2007). Oddly

enough all the proteins encoded by the genes mutated in cystic kidney diseases are localized to the primary cilium of kidney epithelial cells, this includes Glis2. Finally, Glis2 is a paralog of another Hh inhibitor, Gli3, whose activity is dependent on primary cilia (Masetti et al., 2017).

Discussion

Through the DEXSeq we were able to confirm that there are in fact proteins that are being affected in the mutant mouse model that otherwise would not be in the wild type. All of these proteins have been associated with the production of primary cilia in some way. This supports evidence that Prpf8's inability to interact with Dzip1 is detrimental for ciliogenesis. This further indicates that Prpf8 is not functioning as it would under normal regulations. These proteins that are being alternatively spliced give us an understanding on what the key players are on our proposed Dzip1 mechanism. Although the western blot application does not definitively confirm alternative splicing in the probed ciliary targets. It certainly suggests this is a possibility. In future experiments alternative splicing can be confirmed by reverse transcriptase polymerase chain reaction (RT-PCR) and can be used to also determine a plausible connection involving all moving parts identified thus far.

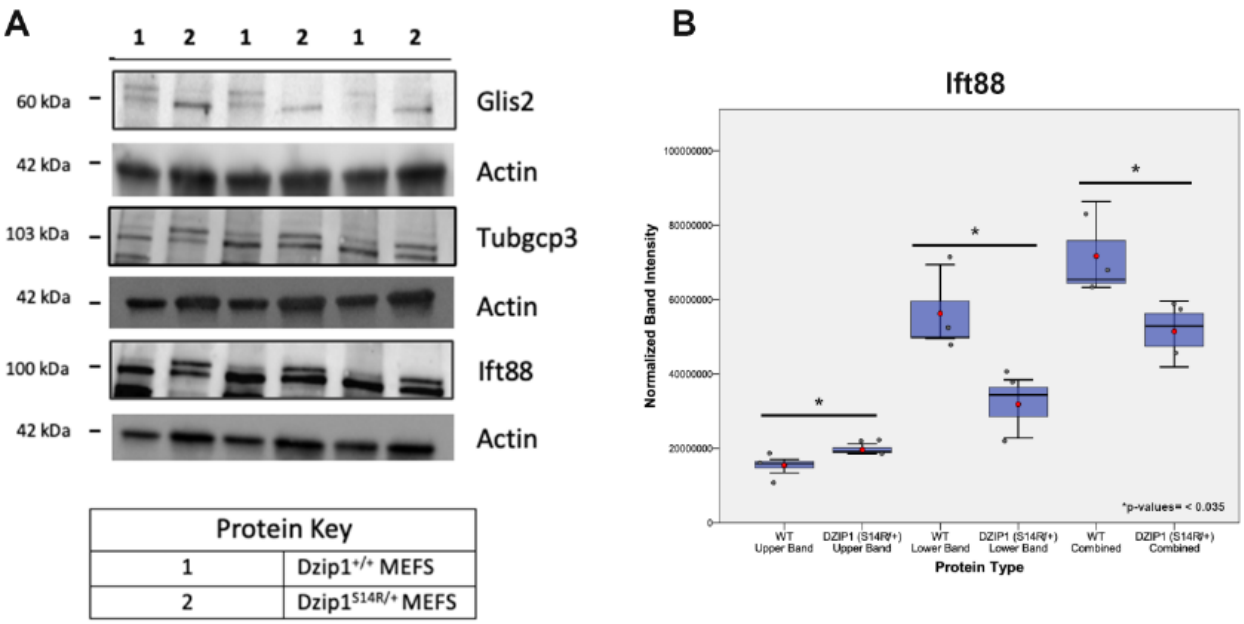

Figure 3.5 Ciliary Targets Have a Difference in Isoforms in Dzip1$^{+/+}$ Compared to Dzip1$^{S14R/+}$ in Mouse Embryonic Fibroblasts. (A) Western Blot Analysis was performed on protein taken from *Dzip1*$^{+/+}$ and *Dzip1*$^{S14R/+}$ mouse embryonic fibroblasts (MEFs). "1" = wild type *Dzip1* MEFs and "2" = *Dzip1*$^{S14R/+}$ MEFs. Dzip1 blots were probed with respective antibodies Glis2, Ift88 and Tubgcp3 (1:1000) n= 3. **(B)** Quantification of Ift88 shows significance in band intensity in *Dzip1*$^{+/+}$ and *Dzip1*$^{S14R/+}$ MEFs. *p-values= <0.035.

CHAPTER 4: MVP GWAS UNCOVERS POSSIBLE ENHANCER

Introduction

Non-syndromic MVP affects between 2-3% of the world's population and there have been recent studies that question the genetic heterogeneity of MVP. The current findings of linked loci to the (Disse et al., 1999) disease and previous family studies that indicate rare connective tissue syndromes (Holbrook & Byers, 1989) verify that MVP is a disease that can be characterized by the mutations of multiple genes. Thus far in the project we have focused our studies on the large family with non-syndromic MVP, which gives us a high-effect because of how rare the point mutation is in the general population. Yet we have neglected to see whether or not there is a link between MVP, DZIP1 and PRPF8 given a larger sample size (lower effect size). Therefore, we reexamined many of the findings from an MVP GWAS conducted on the general population. First, a GWAS Meta-analysis (Table 4.1) was conducted including 1,412 MVP cases and 2,439 controls. Through this study there were 6 significant loci found.

As previously mentioned, genes TNS1 and LMCD1 were the first two significant loci and both came with supported scientific evidence that showed knockdown of LMCD1 led to mitral regurgitation and *Tns1*$^{-/-}$ mice showed myxomatous degeneration in the posterior leaflet. The third most significant locus was SMG6 and to date there had been no known significant data that ties an MVP phenotype to SMG6. Additionally, scientists have discovered that knockdowns of SMG6 in zebrafish exhibit no valvular phenotype (Dina, et. al 2015). By further examination it was discovered that SMG6 resides on chromosome 17. This information was particularly interesting because PRPF8 is located on chromosome 17 as well. Furthermore, the MVP SNP is positioned in the SMG6 intron and it is in close proximity to the PRPF8's gene locus, approximately

500bp (Figure 4.1). This led us to hypothesis that this MVP SNP could be acting as an enhancer for Prpf8.

In a normal reaction that involves the expression of a gene, there is an enhancer and the enhancer's responsibility is to properly interact with the promoter site (specifically the transcription start site) and effectively turn the gene "on". However, the enhancer will not be able to perform its job correctly if there is a mutation inhibiting its correct function. Therefore, the interaction is lost, and the gene will be "off", stopping any regulation of the gene. Furthermore, we completed a luciferase assay to test whether the putative enhancer had any capabilities for enhancer activity. In addition, our collaborators at INSERM completed a 3C experiment, where they were able to isolate four regulatory sequences that are spaciously close to PRPF8's TSS.

Table 4.1 Clinical and Genotyping Features of the Study Populations. The table illustrates the study design behind the GWAS. The study design with cohorts in discovery and follow-up and filtration strategy of SNPs (Dina, et al. 2015) ©

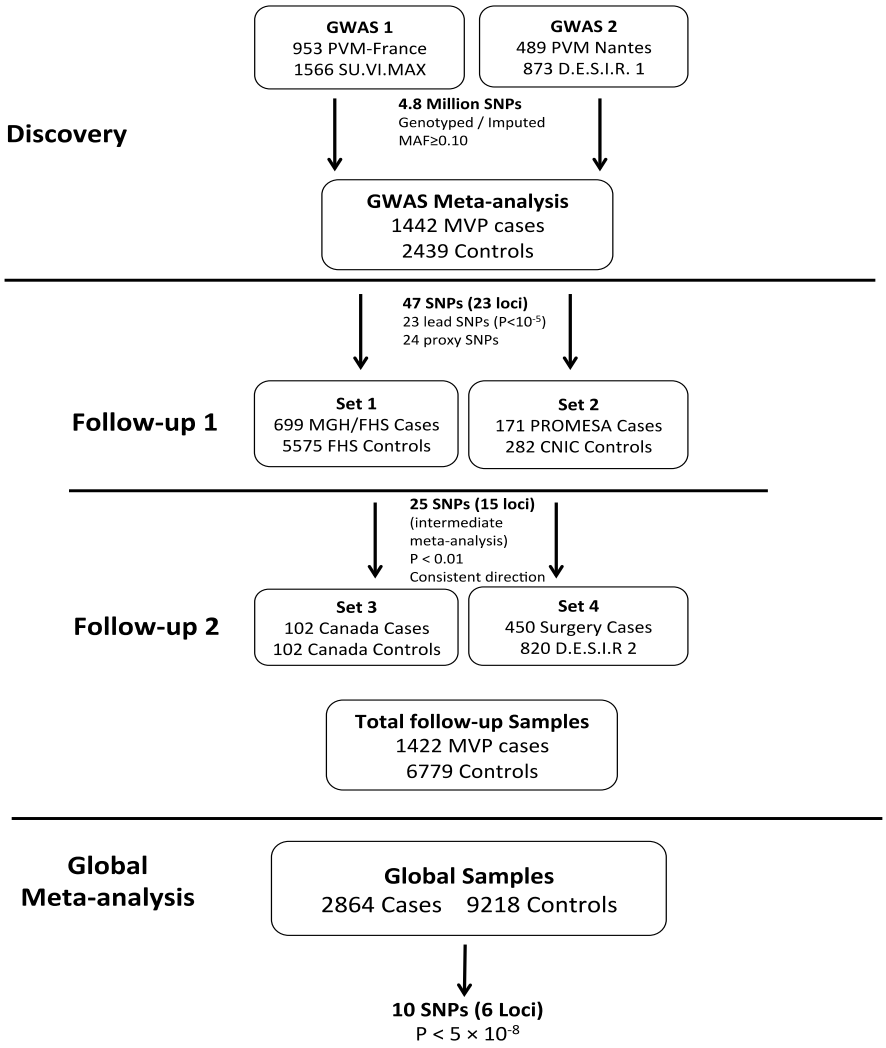

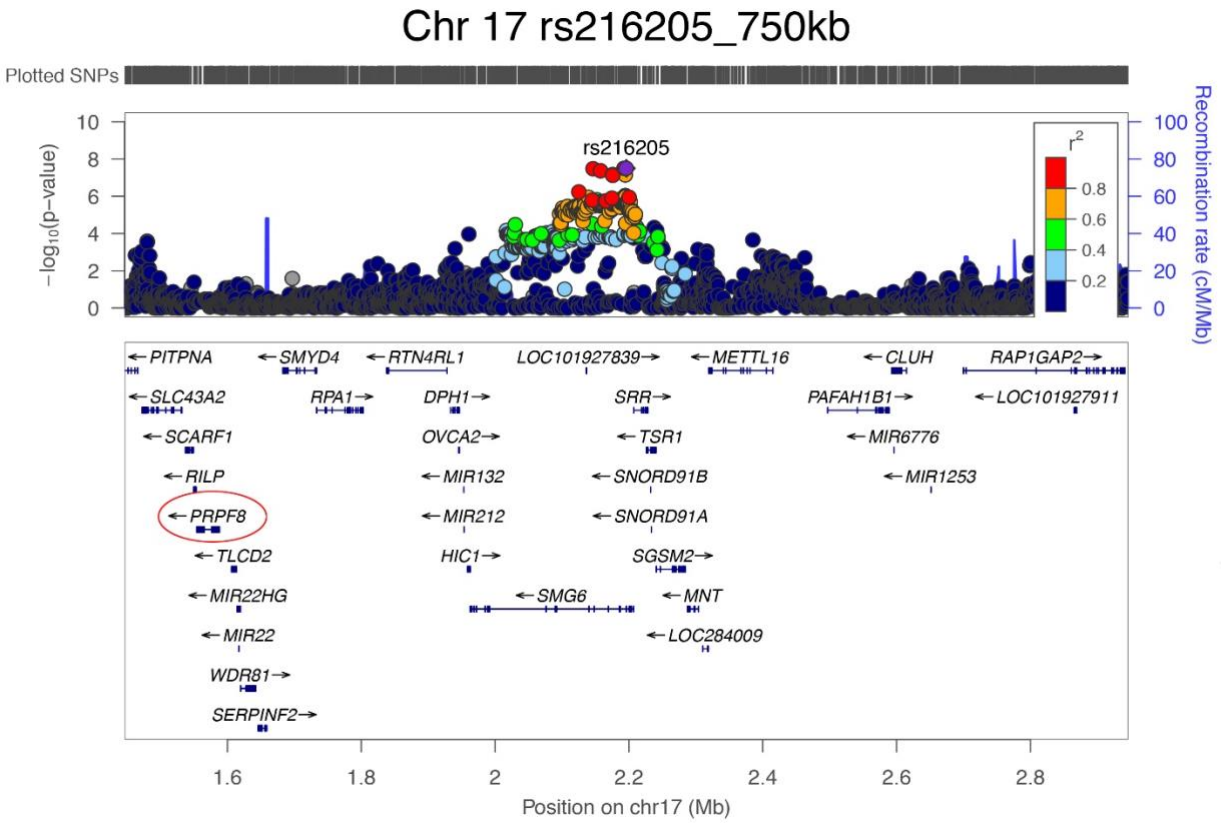

Figure 4.1 Genomic Context of the Association Signal Observed in MVP GWAS Meta-Analysis on Chr17p13. Prpf8 is circled in red. SMG6 is located below thhe position of the MVP SNP is denoted as rs216205 (purple dot) (Image by Nabila Bouatia-Naji and Sergiy Kyryaachenko, Paris Cardiac Research Center)

Results

"Silencer" Identified

Primers were designed to include the correct wild type sequence of the genetic variant found on chromosome 17 (Table 4.2). Once this was found we amplified the sequence and performed a ligation to fuse both the insert and the pre-cut PGL2- promoter vector. The vector backbone contained a *luc* gene, which would be expressed if there was any enhancer activity detected in the insert (MVP SNP- wildtype). Next, we performed a transformation and sequenced the positive colonies to ensure that we had the accurate sequence. Transfections were followed on chicken valvular interstitial cells (cVICs) and human embryonic kidney cells (HEK293T), where they were completed in triplicates and repeated three times. The luciferase assay was performed 48 hours after transfection to measure for enhancer activity.

The results significantly showed that the putative enhancer was in fact showing activity that resembles a repressor (Figure 4.2). This indicates that in normal conditions the wild type variant is a "silencer". There are future experiments that need to be completed to show the activity of the MVP SNP once cloned into the PGL2-promoter vector, this would give us better understanding on how the enhancer could be affecting PRPF8 regulation. Additionally, each insert (MVP SNP and MVP SNP wildtype) need to be cloned into a PRPF8 vector and measure its level of enhancer capabilities under more relevant conditions. Therefore, we would be able to determine each insert's characteristics and conclude whether or not they align to the results found in the PGL2-promoter vector backbone.

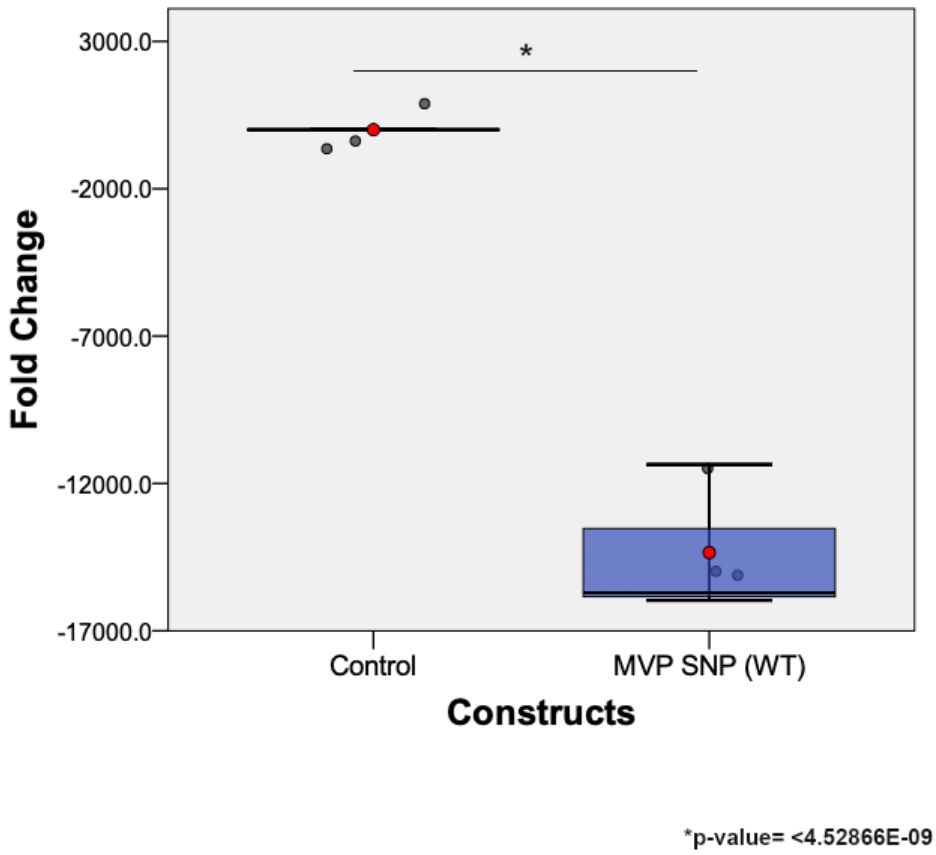

Figure 4.2 Silencer Identified. HH31 chicken valvular interstitial cells ($10X10^5$ cell count) were transfected with the PGL2 promoter reporter and insert constructs labeled sense orientation and antisense orientation, pGFP and PGL2 promoter vector alone for a control. Each plate was treated with bGal to normalize the rate of transfection. After 72 hours, plates were examined and assayed using the Promega Luciferase Assay Kit. **(A-C)** Each graph shows triplicate series performed. **(D)** Compiled data from three series of assay data. (P-values indicated as *=0.187101108 and **= 0.0000019663) n=9.

Potential Regulatory Sequences

In order to take the task on to finding the enhancer that directly interacts with the TSS for PRPF8. Our collaborators in INSERM performed a Chromosome Conformation Capture (3C) experiment. This pioneering technique is able to analyze significantly long range looping interactions between any pair of selected genomic loci (Naumova, et. al 2012). This experiment tested physical interactions between genomic sequence containing the most associated SNP with MVP at Chr17 (rs216205), and several genomic points at variable distance from the SNP that interact with the TSS of PRPF8. This was performed in two separate libraries: dermal fibroblasts and heart fibroblasts. While analyzing the result from the 3C experiment it is determined that there are three regulatory sequences that are in direct contact with the TSS of PRPF8 (Figure 4.3).

In contrast to linear genomic DNA**,** close points were amplified but not distant points. The presence of an amplified sequence on lane 6 indicates the TSS region of PRPF8. Lanes 1, 2 and 3 tested positive for interacting with the TSS region of PRPF8 (Figure 4.4). A fourth sequence was found based off of information obtained from a computer data basis that showed that it is a possible enhancer for PRPF8 (Figure 4.3). Additionally, sequences 1-3 were all short distances from the found MVP SNP (rs216205). Sequence 1 is 75kb away from the MVP SNP followed by sequence 2 which is 93kb from the MVP SNP and finally sequence 3 is 116kb from the MVP SNP. Given the original size of each sequence found an Assay for Transpose-Accessible Chromatin with high-throughput sequencing (ATAC-seq) was performed to ultimately condense the size of each sequence to approximately 200bp by performing amplifying the open

chromatin with the use of the enzyme transposase (Shrestha, Ding, Jones, & MacLean, 2018).

Primers were designed for all four sequences (Table 4.3) and they were cloned into the PGL2-promoter vector and examined for enhancer function, through ligation and transformation steps (Figure 4.5).

The sequences were transfected into HEK293T cells, due to the fact that HEK293T cells can be easily transfected and they are a part of the human genome, making all sequences cloned 100% conserved. A luciferase assay was conducted to measure enhancer activity. The measurements and quantifications are listed (Figure 4.6). Through this application we were able to decipher which sequences had enhancer capabilities. We were fortunate enough to clone in the mutation for the 1st regulatory sequence and apply this to our theory. This resulted in confirming that the 1st regulatory sequence had significant enhancer capabilities compared to the PGL2 promoter vector. The remaining sequences (2,3 and 4) were ruled out as they did not exhibit any significant enhancer activity. This finding gives us insight on how PRPF8 is being regulated in the presence of the Dzip1 point mutation. Furthermore, in addition to the previous "silencer" found and both versions of sequence 1 (mutation and wild type) need to be cloned into a PRPF8 vector backbone to test for enhancer activities in the presence of the PRPF8 TSS and determine whether each sequence of 1 and the repressor carry the same behavior seen in the PGL2 promoter vector.

Discussion

Each sequence tested gave us a closer look into the various possible reasons as to how the regulation of Prpf8 is being affected in the presence of the *Dzip1*$^{S14R/+}$ mutation.

The significant findings of the repressor in the wild type version of our MVP SNP indicated that there may be a series of events unfolding that are untraditional in the sense that in normal settings there is a detected “silencer” in close proximity to the TSS of PRPF8. As stated earlier, further studies need to be completed that show a definitive significant change in either of the sequences compared to the lone PGL2-promoter vector. Furthermore, we were able to verify enhancer capabilities by cloning each sequence into the PGL2 promoter vector. Yet, in order to understand the nature of PRPF8’s regulation the enhancer needs to be cloned with a PRPF8 backbone. Our previous studies are promising as it laid the groundwork for future experiments and knowledge regarding the mechanism behind Dzip1 in MVP patients.

Table 4.2 SNP Region Cloned. Primer sequences used for Cloning/Sanger Sequencing MVP SNP (rs216205) region.

Primers used to isolate MVP SNP region		
Primer Name	Forward Primer	Reverse Primer
MVP SNP (wild type)	5'-CTAGGTACCGGGAGCAAGCC-3'	5'-AGCAATGTGCTGGGCCTTC-3'

Table 4.3 Potential Regulatory Sequences. Primers for potential regulatory sequences found through 3C experiment.

Potential Regulatory Sequences		
Sequence	Forward Primer	Reverse Primer
Regulatory Sequence 1	5'-CTA AAT TCT GCA GTG ACA CA-3'	5'-AAT GAT GCA ATG AGC CAA AC-3'
Regulatory Sequence 2	5'-TGC CCT GGG AAG ACC GTG GA-3'	5'-GAG CCA CCA CAC CAG GCC AT-3'
Regulatory Sequence 3	5'-CTA CAA TCC GGC TTC CAG TT-3'	5'-TGA TAC AGG TGG TGG TTG AA-3'
Regulatory Sequence 4	5'-AGA GAA AGA ACT ATT TGA AG-3'	5'-TTC GAA ACT GCA AGG AAT GG-3'

A. >hg38_dna range=chr17:2282433-2282633 5'pad=0 3'pad=0 strand=+ repeatMasking=none

CTAAATTCTGCAGTGACACATAGTGGTGAGAGAGGGAAGTACATAATAAAGATAAAGGAAGCGTACATG
AGAAGGGAAAAGACCATCAGGGAGCCTCAAGTGGTTTGTCTTCCTTGCAATCAGTGGGAAGTATCTGTGC
CTCACAGCTGTATGAACCAGGGCACCCAGGCTTACTGAGCTAGTTTGGCTCATTGCATCATT
Position of rs9899330 is in Red. **Noted as Regulatory Sequence 1**

B. >hg38_dna range=chr17:2282706-2282906 5'pad=0 3'pad=0 strand=+ repeatMasking=none

TGCCCTGGGAAGACCGTGGATGGGATGGATGAATCCAGATCTCCAGGCGAGTGGTGTCATCTCCAACATG
CCGGAAAGTAGACTTCTTTCCTTTCCGCCACTGGTCAGGGCTCAGGTCAAATTCCTCATGTTGCTTCTTTT
CCATCTGTTCTGCCTATATAACATACAAACACATTAGCTCATGGCCTGGTGTGGTGGCTC
Position of rs749240 is in Blue. **Noted as Regulatory Sequence 2**

C. >hg38_dna range=chr17:2295498-2295698 5'pad=0 3'pad=0 strand=+ repeatMasking=none

CTACAATCCGGCTTCCAGTTTCCCCAACTAAATTAACTCTTGATAAGTTCATCCAATCCAACGGACACTTT
TTAGTAATCTTAACATTTGACAGCTCCATTGCACTTGACAATTTTACCTACCCCCACCTTGAAATGTAACC
CCCGTTTCTGGCCAGCCTTCCCAGTACCCCAACTTTTGCTTCAACCACCACCTGTATCA
Position of rs17834627 is in Green. **Noted as Regulatory Sequence 3**

D. >hg38_dna range=chr17:2262320-2262520 5'pad=0 3'pad=0 strand=+ repeatMasking=none

AGAGAAAGAACTATTTGAAGGATTCACTTCTAAGCTTGAGCCAAATCAAAAGCTCAAATCTATCTACATT
GTGATGAATCTTCAGTTCCAACTGAGTGATCAGACAGCACCAATGTGGACATCTGTACCATGGCCCAAGA
CATTATAATGACAGAATCTTGGCTGGGAATCTCAGAAGCAACCATTCCTTGCAGTTTCGAA
Position of rs170040 is in Orange. **Noted as Regulatory Sequence 4**

Figure 4.3 Potential Regulatory Sequences. 3C experiment was completed to determine the sequences with physical interaction to the MVP SNP (rs216205) region and the TSS for PRPF8.

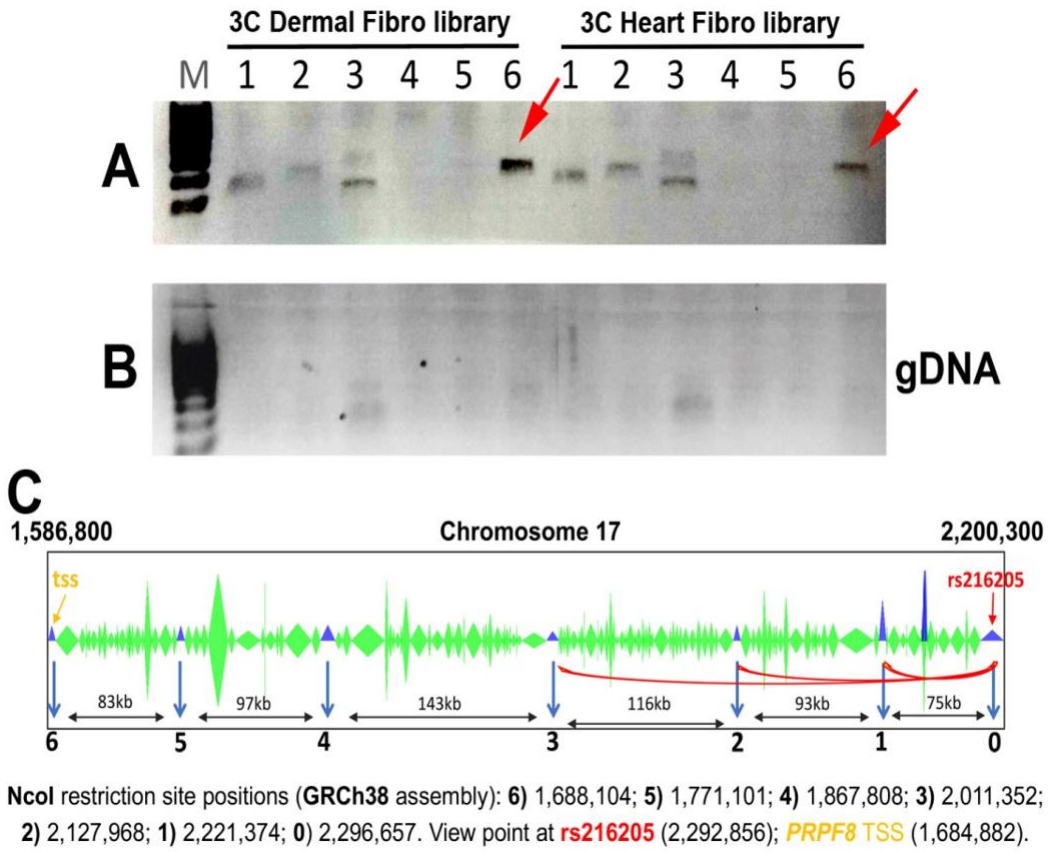

Figure 4.4 Chromatin Conformation Capture of PRPF8 TSS and Potential Enhancers. 3C experiments on Chr17 MVP locus. **(A)** Chromatin conformation capture from two separate libraries (dermal and heart fibroblasts) tested physical interactions between genomic sequence containing the most associated SNP with MVP at Chr17 (rs216205), and several genomic points at variable distance from the SNP. In contrast to linear genomic DNA **(B)**, close points were amplified (lanes 1, 2, positive controls) but not distant points (lanes 4 and 5, negative controls). The presence of an amplified sequence on lane 6 indicates that despite the linear distance between the 2 points (600Kb), the SNP and the TSS region of PRPF8 are close in the native chromatin that we captured through the 3C experiment. **(C)** Chr 17 locus with segments (1-6) that were tested in 3C libraries. PRPF8 transcription start site (tss) is denoted in yellow (Image by Nabila Bouatia-Naji and Sergiy Kyryaachenko, Paris Cardiac Research Center).

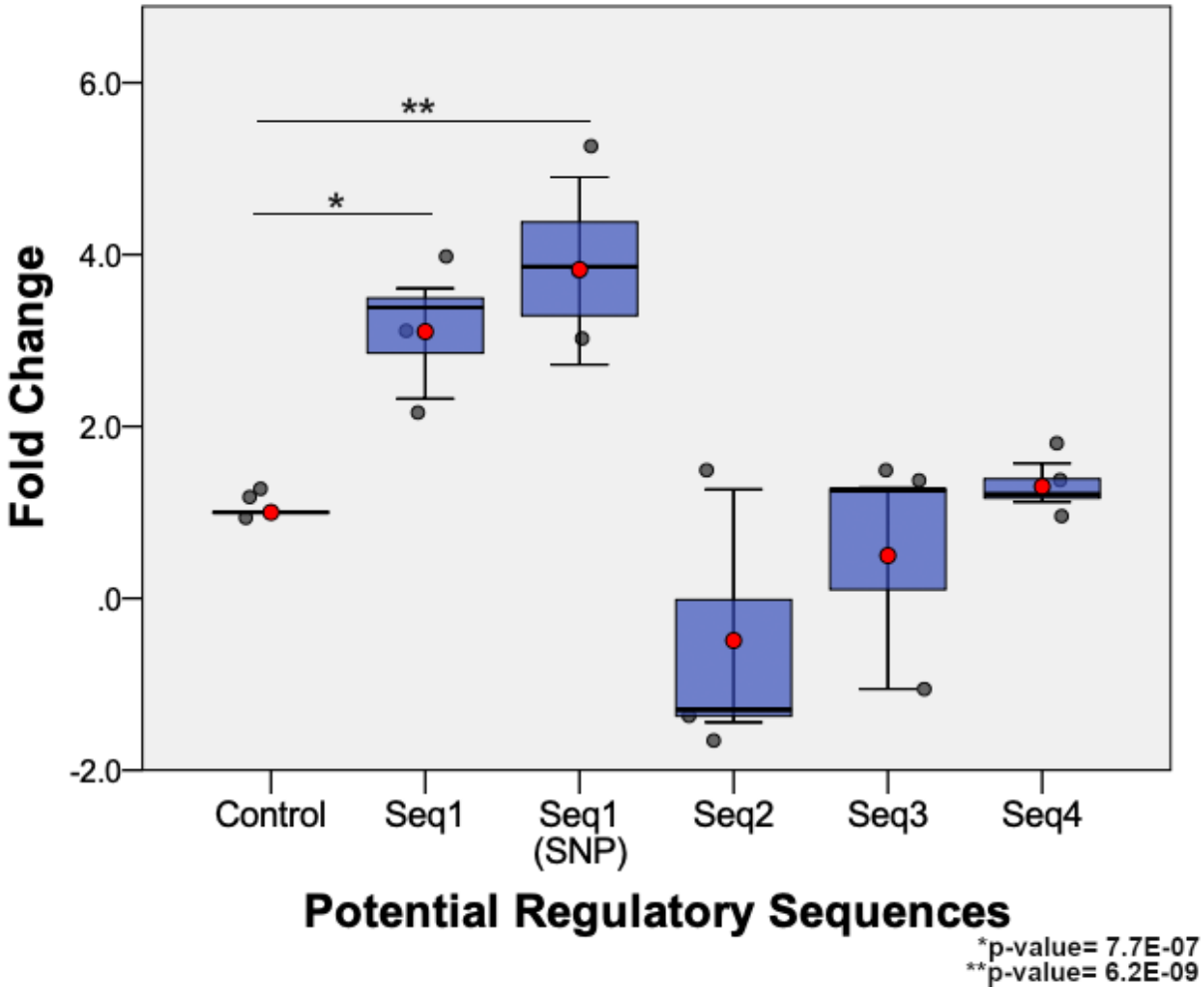

Figure 4.5 Luciferase Assay Measures Enhancer Capabilities in Potential Regulatory Sequences. All potential sequences were cloned and tested for RLU levels in comparison to PGL2 vector. 1st Regulatory Sequence (mutation) A had significant fold change and RLU levels. Antisense of 1st sequence was cloned to compare the mutation in Regulatory Sequence A to its respective wild type.

CHAPTER 5: OVERALL DISCUSSION

Overall Discussion

Mitral valve prolapse is one of the most common cardiac diseases, affecting on average 3 million people nationwide. The function of prolapsed valves results in regurgitation, arrhythmias and even sudden cardiac death in severe cases. The phenotype of these valves includes myxomatous degeneration, resulting in an increase in proteoglycans, fragmented collagen and hyperplasia.

Currently invasive surgery is the only option to replace or repair the valves. While the etiology of this disease is still not fully understood, studies within our lab suggest that primary cilia play a critical role in the valve disease.

Primary cilia have been found to play a central part in valvular development as mutations that disrupt the formation of primary cilia lead to improper valve development. This is due to the role that cilia have been proven to regulate cell cycle, proliferation and matrix deposition. Studies show that signaling through them regulates ECM production, while current studies are providing more insight on hedgehog signaling being the main pathway for this.

Primary cilia are temporally expressed on the leaflets of the mitral valve and are noticeably absent at adult timepoints. This indicates that they are essential for early stage development. This begs the question, why do we see this diagnosis of MVP in adults rather than when cilia are actually present on the valve?

Overall, as the patients ages, the enlarged postnatal leaflets cause the endothelial borders to stretch, causing breaks that allow for a cytokine release and infiltration of extracardiac cells, furthering the enlargement of the valves and thus causing valves to lose normal function.

Over the past few years scientists have strived to investigate the mechanisms by which primary cilia contributes to valve disease. Our hypothesis proposed at the beginning of this project was that the Dzip1 regulation of ciliogenesis through a Prpf8 mRNA splicing mechanism is broadly involved in MVP disease. The studies previously outlined looked to test whether adequate data could be collected to support this.

By establishing that both Prpf8 and Dzip1 were co-localized and co-expressed together on the mitral valve serves as a foundation to the previous studies. This evidence supports the findings from the two-hybrid screening and from the data collected we propose the following working model.

As it has been stated primary cilia serve as mechanosensors for the cell and signaling through them has been shown to regulate cell cycle, proliferation, and migration. Recent studies within our lab show that defects in primary cilia have a higher prevalence for MVP. This association has led to several genetic studies that link mutations in *DZIP1* to many MVP patients. Dzip1 experiences many different interactions but one stood out in particular, Prpf8 as it was the only protein that was unable to bind to DZIP1's mutant plasmid in a two-hybrid screening.

Furthermore, the mutation in Dzip1 disrupts Prpf8's job to splice mRNAs encoding proteins that affect the process of ciliogenesis, i.e. Ift88. Ift88, a centrosomal protein that is required for the building of cilia shows evidence of being alternatively spliced. Other ciliary proteins that have a difference in splicing isoforms are: Tubgcp3 and Glis2.

By investigating the interaction of PRPF8 and DZIP1 we were determined to take a closer look at what could be enhancing the regulation of PRPF8. We examined many different potential enhancers. First we found that there was an MVP SNP in close

proximity to PRPF8's locus that could be affecting the regulation of PRPF8. The wild type sequence of the MVP SNP was cloned first into the PGL2 promoter, and it exhibited 'silencer" activity. Second, additional potential regulatory sequences were identified through the 3C experiment which tested the location surrounding the MVP SNP and if there was any direct physical interaction between it and the TSS of PRPF8. The work completed has the ability to directly influence therapies for MVP.

Furthermore, as we look at the cycle of discovery between MVP, DZIP1 and PRPF8, we examine them from two different perspectives. The first from a large non-syndromic family with MVP exhibiting a significantly rare point mutation in DZIP1 not commonly seen in the general population. The second from a broader perspective that involves examining the general population as a whole to investigate whether there is a common link between MVP, DZIP1 and PRPF8 in a larger sample size with a low effect size (Figure 5.1).

Future studies are needed to further find the direct mechanism by which mutations cause valve disease, but studies performed in the project have increased the understanding behind genetic alterations in MVP. Therapeutic aids are promising, such as developing one to target the reduction of further degradation or to provide complete function of the spliceosome in the presence of a point mutation as it relates to this research could result in non-invasive treatment for patients with MVP. The data provided gives us an understanding of the cellular and molecular cause of MVP as it relates to primary cilia and the genetic information that supports this hypothesis. Finally, the research presented specifies a broad mechanism by which mutations in Dzip1, a centrosomal protein needed

for ciliogenesis inhibit the proper function of Prpf8, a central component of the spliceosome.

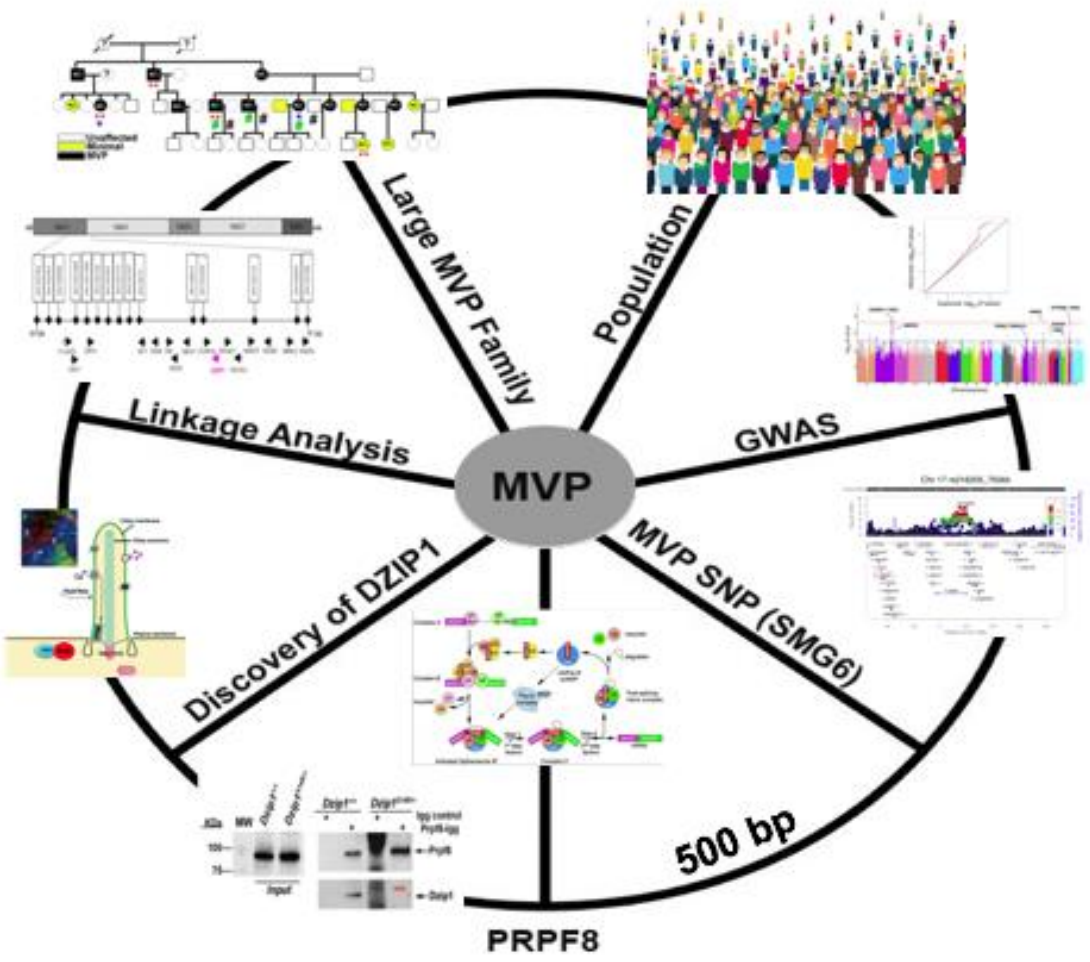

Figure 5.1 The Cycle of Discovery. Schematic diagram of the two perspectives taken in linking MVP to both DZIP1 and PRPF8.

CHAPTER 6: MATERIALS AND METHODS

Mouse Studies

All mouse experiments were performed under protocols previously approved by the Institutional Animal Care and Use Committee (IACUC) at the Medical University of South Carolina. Prior to cardiac resection, mice were euthanized in accordance with the Guide for the Care and Use of Laboratory Animals (NIH Publication No. 85-23, revised 1996.) Comparisons between sexes were evaluated and no significant differences were observed. As such, data is comprised of pooled sexes for all experiments.

Dzip1 knockin mice

Dzip1 knockin mice were generated through CRISPR technology.

Scientists were able to take the exact Dzip1 point mutation that we found in patients with MVP into a mouse model. Founder lines 731 and 736 were utilized in the studies listed throughout this project. Mating strategies were as follows. Founder lines: 731 and 736 are both male and are genotyped to be heterozygous for the point mutation. The lines were mated with female C57/B6 mice from JAX Laboratories. Mice resulting from these mating would be either wildtype or heterozygous for the $Dzip1^{S14R/+}$ point mutation, resulting in an F1 generation. F2 generations were outbred as well in the same manner with male heterozygous mice and female wildtypes. All mice were inbred. The knockin mutant allele was genotyped using forward primer: 5'-CATCAGAGGCTCACGAGGAG-3' and reverse primer 5'-GCGTGGACAGCATCTTCTTC-3'. Histology was performed on embryonic and adult wild type ($Dzip1^{+/+}$), heterozygous ($Dzip1^{S14R/+}$) and homozygous ($Dzip1^{S14R/S14R}$) hearts on mixed background.

Dzip1 conditional mice

Conditional knockout mice were generated by a targeted homologous recombination approach using a Dzip1 targeting construct (PG00125_Z_2_E04) purchased from the KOMP mouse repository. The conditional knockout would delete exons 8 and 9 (Dzip1-202 transcript) and cause a reading frameshift and premature translational termination. The conditional mutant allele was genotyped using forward primer: 5'-GCCAAAGTGGTTTGCCTGACA -3' and reverse primer: 5'-GCAGGTTAAACACTCATATAGC-3'.

IFT88 conditional mice

Ift88 conditional mice and genotyping were previously described (Haycraft, Zhang et al. 2007). Histology was performed on embryonic and adult wild type (NfatC1Cre-;Ift88f/f) conditional heterozygous (NfatC1Cre-;Ift88f/+) and conditional knockout (NfatC1Cre+;Ift88f/f) hearts on mixed background.

Histology, Immunohistochemistry/Immunofluorescence

Embryonic and adult tissue were processed for immunohistochemistry/ immunofluorescence (IHC) from Dzip1 knock-in mouse models (wildtype, heterozygous and homozygous). IHC staining was performed on 5 um thick sections from embryonic stages: E11.5, E13.5, E15.5 and P0 mitral valves. For immunohistochemistry (IHC): Antigen retrieval was performed for 5 minute using antigen unmasking solution (Vector Laboratories, Burlingame, CA, USA, Cat#H-3300) by pressure cooker (Cuisinart,

Stamford, CT, USA). The following are the antibodies and their dilutions; Acetylated Tubulin (Sigma, Cat#T6793, 1:500), Gamma Tubulin (Abcam, Cambridge, MA, USA, Cat#ab11317, 1:1000), Dzip1 (Santa Cruz, Cat#SC: 515454, Medical University of South Carolina, 1:250), Prpf8 (Abcam, Cambridge, MA, USA, Cat#ab185547 1: 50). Primary antibody was detected using fluorescent secondary antibody, Goat anti-Mouse IgG Alexa fluro 488 (Cat#A-11029, 1:100), Goat anti-Rabbit Alexa fluor 488 (Cat#A-11034, 1:100) anti-Mouse Alexa fluor 568 (Cat#A-11004,1:100), anti-Rabbit Alexa fluor 568). Nuclei were counterstained with Hoechst (Life Technologies, Cat#H3569, 1:10,000) for 10 minutes and slides were coverslipped with SlowFade mounting medium (Life Technologies, Cat#S36937). Fluorescence imaging was performed using Zeiss Axioimager M2 and Leica TCS SP5 AOBS Confocal Microscope System.

Confocal Microscopy

Images were acquired using the Leica TCS SP5 AOBS Confocal Microscope System (Leica Microsystems, INc., 410 Eagleview Boulevard, Suite 107, Exton, PA 19341). Z-stacks were set by finding the highest and lowest depth with visible fluorescence and using the system optimized setting to determine steps. Z- stacks were then compiled to form maximum projection images.

3D reconstruction

3D reconstructions of H and E images were performed to generate volumetric measurements of postnatal day 0 right, left, and non-coronary leaflets, similarly to

previous reports. Images were then aligned using ImageJ FIJI and imported into Imaris 8.0. Manual reconstruction was performed by tracing each individual cusp on every section and combining all traces to create a 3D structure. Additionally, 3D reconstructions of immunohistochemistry were performed by importing Z-stack images of 15**μ**m sections into Imaris and creating surface renderings based on intensity of the stains.

Cell Culture

Hek293T and cVICs cell lines were ordered from Thermo Fisher. Adult tail fibroblasts were generated from Dzip1 knockin tail snips (genotypes: wildtype, heterozygous and homozygous) at ages ranging between 2-4 months old. Hek293T, cVICs and adult tail fibroblasts were cultured in a 37 degree Celsius, 5% CO_2 incubator, all in their respective media. Hek293T and Adult Tail Heks and fibroblasts cells were incubated in DMEM/ High Glucose media (Corning™ DMEM with L-Glutamine and 4.5g/L Glucose; without Sodium Pyruvate, cat#10-017 CV), with 10% fetal bovine serum (FBS) (XYCellCulture, cat #FBS-500, Kansas City, MO) and 1% Penicillin/Streptomycin mixture (Life Tecnologies, cat#15070-063 Carlsbad, CA). cVICs were incubated in Medium 199/EBSS media (Hyclone™+ Earle's Balanced Salts+ L-Glutamine), with 10% chicken serum (Bio-World, cat#30611183-11 Dublin, OH) and 1% Penicillin/Streptomycin mixture (Life Tecnologies, cat#15070-063 Carlsbad, CA) Media on the cells were changed every 2-3 days and cells are passaged by using 0.05% EDTA trypsin when plates were $\leq$ 90% confluent.

Protein extraction and Western Blot Analysis

Protein from adult tail fibroblasts was extracted by lysis of cell pellets with RIPA buffer and protein concentrations are determined by performing a Bradford Assay as per the manufacturer's instructions. 100ug protein of each sample was then separated on an SDS-PAGE gel and transferred to a BioRad membrane (Trans-Blot Turbo: Transfer System) using the BioRad western blotting system (BioRad, Hercules, CA). Membranes were blocked using 5% milk in 1X TBST for 1 hour and then probed overnight, at 4 degree Celsius on a rotator. The following are the primary antibodies at 1:1000 dilutions: Dzip1 (gift from Stan Hoffman, Medical University of South Carolina, 1: 250), Ift88 (Millipore, MA, USA, Cat#ABC932), Tubgcp3 (Millipore, MA, USA, Cat#ABC932) and Glis2 (Novus Biological, Centennial, CO, USA, Cat# NBP2-41311). The membranes were then washed with 1X TBST five times, 10 minutes each and then incubated for 1 hour with secondary antibodies at room temperature. The secondary antibody, Anti-Rabbit IgG HRP (Abcam, Cambridge, MA, USA, Cat#A9169), was used at 1:10,000 dilution. Membranes were then washed again in TBST 5 times, for 10 minutes each. ECL solution was then added for 5 minutes (West Femto, Fisher Scientific, Hampton, NH). Signals were then detected using ChemiDoc MP Imaging System (Medical University of South Carolina :3193950)

End-Conversion/Ligation/Transformation

Assemble the following components in a 0.5 ml tube (add the End Conversion Mix last): 0.5–2.0 µl PCR product (or 2 µl Blunt Vector Control Insert; *see note below) X µl Nuclease-free Water to a total of 10 µl 5.0 µl End Conversion Mix 10 µl total volume Mix gently by stirring with a pipet tip. * Set up a positive control to test the efficiency of

the vector: substitute 2 µl (9 ng = 0.067 pmol) of the Blunt Vector Control Insert provided with the kit in place of the amplified product in the above end conversion reaction. The Blunt Vector Control Insert is a 212 bp PCR product amplified with Taq DNA polymerase. Also prepare a negative control, omitting the PCR product or control insert. Incubate the end conversion reaction at 22°C for 15 min. Inactivate the reaction by heating at 75°C for 5 min. Note that complete inactivation of the kinase in the End Conversion Mix is required to avoid high vector background. Cool the reaction briefly on ice (2 min). Please note that the reaction must be chilled prior to proceeding to the ligation step to avoid inactivating the ligase. Briefly centrifuge the cooled reaction to collect the condensate and proceed to the ligation reaction. Ligation For a standard reaction, 1 µl (50 ng) Blunt Vector and 1 µl (4 U) T4 DNA Ligase are added directly to the End Conversion reaction, which brings the total volume to 12 µl. To the cooled End Conversion reaction, add 1 µl Blunt Vector, and then 1 µl T4 DNA Ligase. Mix gently by stirring with the pipet tip used to add the ligase. Incubate at 22°C for 15 min. The molar ratio of insert to vector is 2.5:1 under these conditions. This ratio has been shown to produce maximum efficiency for ligation to the Blunt Vector Positive Control 212 bp insert. Using insert to vector molar ratios from 1:1 to 2.5:1. Treat the positive and negative controls set up in the End Conversion step in exactly the same manner as the insert-containing sample. Perfectly BluntTM Cloning Kits 8 Novagen TB183 11/99 United States & Canada 800-207-0144 Germany 0800 6931 000 United Kingdom 0800 622935 Transformation of NovaBlue Singles™ Competent Cells For transformation, 1 µl of the ligation reaction is added directly to NovaBlue Singles Competent Cells. Adding higher amounts of the ligation reaction generally will not produce more transformants;

more than 2 µl of ligation reaction can dramatically inhibit transformation. Note: Upon receipt from Novagen, verify that the competent cells are still frozen and that dry ice is still present in the shipping container. Immediately place the competent cells at –70°C or below. For optimal results, do not allow the cells to thaw at any time prior to use. Handle only the very top of the tube and the tube cap to prevent the cells from warming. Keep the cells on ice whenever possible. To mix cells, flick the tube 1–3 times. Do not vortex the competent cells. Remove the appropriate number of tubes of NovaBlue Singles Competent Cells from the freezer (include one extra sample for the Test Plasmid positive control, if desired). Immediately place the tubes on ice, so that all but the cap is surrounded by ice. Allow the cells to thaw on ice for ~2–5 min. Visually check the cells to see that they have thawed and gently flick the cells 1–2 times to evenly resuspend the cells. The cells are then ready for the addition of the ligation reaction. Add 1 µl of a ligation reaction or purified plasmid DNA (~1ng/µl) directly to the cells. Stir gently to mix and return the tube to the ice, making sure that the tube is surrounded by ice except for the cap. Repeat for additional samples. Place tubes on ice for 5 min. Heat the tubes for exactly 30 sec in a 42°C water bath; do not shake. Hold the rack in the water bath so that the lower halves of the tubes are submerged for 30 sec, and then replace the rack on ice. Place on ice for 2 min. 8. Add 250 µl of room temperature SOC Medium to each tube and perform the “outgrowth” step (shaking incubation) for 30–60 minutes and shake at 200-250 rpm at 37°C and plate immediately following this step.

Transfection

Obtain cVICs/HEK293T from the incubator and count on hemocytometer. For this experiment $1X10^5$ cells per well was used. Label well plates accordingly. Plate cells to labeled wells. Do not plate more than 2ml of media and cells combined per well. Label respective tubes 3.5X cocktails with that include: construct and bgal. Label transfection tubes: Add SF Media, Add DNA (cocktail)-respective amount and then Fugene (Promega, cat#E2311, Madison,WI) Add 6ul of fugene into Transfection tubes. Wait 15 min. Examine under microscope. Monitor for 48hr. Then complete luciferase assay.

Co-Immunoprecipitation

Lysates were obtained from adult tail fibroblasts and 100 µL denaturing lysis buffer was added to 0.5–2x107 cells. This was followed by vortexing vigorously for 2–3 sec at maximum speed. The cell suspension is then transferred to a microcentrifuge tube and samples were heated to 95°C for 5 min to denature the mixture. The suspension was diluted with 0.9 mL non-denaturing lysis buffer and mixed gently. To immunoprecipitated the cells add 5 µL of Rb IgG antibody (Invitrogen, Carlsbad, CA USA, Cat#ab31235) to 1 mL of lysate then incubate for 1 hr. on ice. Then 25 µL of bead slurry was added to the lysate and incubated for 10–30 min at 4°C with gentle agitation and spun in microcentrifuge at 14,000 x g at 4°C for 10 min. The bead pellet was disregarded and supernatant kept for the immunoprecipitation. 5 µL of primary antibody, Prpf8 (Abcam, Cambridge, MA, USA, Cat#ab185547) is added to the supernatant. Then incubate the lysate-bead/antibody conjugate mixture at 4°C under rotary agitation overnight. At the end of the incubation, wash steps (5X10min) were given. Centrifuge the

tubes, remove the supernatant from the beads and discard. Wash the beads with washing buffer or lysis buffer three times to remove non-specific binding. For each wash, mix the beads gently with wash buffer, centrifuge at 4℃ and discard the supernatant.

Luciferase Assay

Promega Luciferase 100 assays E1500 kit. Prepare Luciferase Assay Reagent (LAR) by adding Luciferase Assay Buffer (10ml for E152A and 100ml for E152B) to the vial of lyophilized Luciferase Assay Substrate. Dispense into working aliquots and store unused LAR at –20°C or –70°C. Before each use of the system, allow LAR to equilibrate to room temperature. (Do not thaw LAR at temperatures above 25°C.) Prepare 1X lysis reagent by adding 4 volumes of water to 1 volume of 5X lysis reagent (Cell Culture Lysis Reagent [CCLR], Cat.# E1531; Reporter Lysis Buffer [RLB], Cat.# E3971. Remove growth medium from cultured cells. Rinse cells in 1X PBS. Do not dislodge cells. Remove as much of the final wash as possible. Dispense a minimal volume of 1X lysis reagent (CCLR, RLB or PLB) into each culture vessel (e.g., 400µl/60mm culture dish, 900µl/100mm culture dish or 20µl/well for a 96 well plate).For culture dishes, scrape attached cells from the dish, and transfer the cells and solution to a microcentrifuge tube. Pellet debris by brief centrifugation, and transfer the supernatant to a new tube. Mix 20µl of cell lysate with 100µl of Luciferase Assay Reagent and measure the light produced. Luciferase assay measured on the Monolight ® 2010, Analytical Luminescence Laboratory (Medical University of South Carolina).

RNA Seq analysis

Mitral leaflets were dissected from P0 NfatC1$_{Cre(+)}$; Ift88$_{f/f}$ and P0 NfatC1$_{Cre(+)}$, Ift88$_{+/+}$. Total RNA was isolated using MicroRNeasy (Qiagen). Purity and quantification was determined by Bioanalyzer. The library preparation was made using the SMART-Seq®v4 RNA-seq kit (Clontech Laboratories, Mountain View, CA) following the manufacturer's instructions.

The analysis was carried out on an OnRamp Bioinformatics Genomics Research Platform (OnRamp Bioinformatics, San Diego, CA). "OnRamp's advanced Genomics Analysis Engine utilized an automated RNAseq workflow to process the data, including (1) data validation and quality control, (2) read alignment to the mouse genome (mm10) using STAR RNA-seq aligner, (3) generation of gene-level count data with HTSeq, and (4) 139 differential expression analysis with DEseq2, which enabled the inference of differential signals with robust statistical power (Dobin, Davis et al. 2013, Love, Huber et al. 2014, Davis-Turak, Courtney et al. 2017). Transcript count data from DESeq2 analysis of the samples were sorted according to their adjusted p-value or q-value, which is the smallest false discovery rate (FDR) at which a transcript is called significant. FDR is the expected fraction of false positive tests among significant tests and was calculated using the Benjamini-Hochberg multiple testing adjustment procedure (Benjamini and Hochberg 1995). The DE list was then submitted to the iPathway Guide tool from Advaita® Bioinformatics which uses a systems biology approach in order to identify pathways that are significantly impacted in any condition - from high-throughput gene expression data. The impact analysis incorporates the classical probabilistic component of the magnitude of the expression changes of each gene, the position of the differentially expressed genes

on the given pathways, the topology of the pathway that describes how these genes interact, and the type of signaling interactions between them (Draghici, Khatri et al. 2007).

REFERENCES:

Ansley, S. J., Badano, J. L., Blacque, O. E., Hill, J., Hoskins, B. E., Leitch, C. C., . . . Katsanis, N. (2003). Basal body dysfunction is a likely cause of pleiotropic Bardet-Biedl syndrome. *Nature, 425*(6958), 628-633. doi:10.1038/nature02030

Attanasio, M., Uhlenhaut, N. H., Sousa, V. H., O'Toole, J. F., Otto, E., Anlag, K., . . . Treier, M. (2007). Loss of GLIS2 causes nephronophthisis in humans and mice by increased apoptosis and fibrosis. *Nat Genet, 39*(8), 1018-1024. doi:10.1038/ng2072

Barlow, J. B., & Pocock, W. A. (1963). The significance of late systolic murmurs and mid-late systolic clicks. *Md State Med J, 12*, 76-77.

Beales, P. L., Bland, E., Tobin, J. L., Bacchelli, C., Tuysuz, B., Hill, J., . . . Scambler, P. J. (2007). IFT80, which encodes a conserved intraflagellar transport protein, is mutated in Jeune asphyxiating thoracic dystrophy. *Nat Genet, 39*(6), 727-729. doi:10.1038/ng2038

Bellhouse, B. J., & Reid, K. G. (1969). Fluid mechanics of the aortic valve. *Br Heart J, 31*(3), 391.

Bruckner, A., Polge, C., Lentze, N., Auerbach, D., & Schlattner, U. (2009). Yeast two-hybrid, a powerful tool for systems biology. *Int J Mol Sci, 10*(6), 2763-2788. doi:10.3390/ijms10062763

Buckberg, G. D., Nanda, N. C., Nguyen, C., & Kocica, M. J. (2018). What Is the Heart? Anatomy, Function, Pathophysiology, and Misconceptions. *J Cardiovasc Dev Dis, 5*(2). doi:10.3390/jcdd5020033

Butcher, J. T., & Markwald, R. R. (2007). Valvulogenesis: the moving target. *Philos Trans R Soc Lond B Biol Sci, 362*(1484), 1489-1503. doi:10.1098/rstb.2007.2130

Butcher, J. T., McQuinn, T. C., Sedmera, D., Turner, D., & Markwald, R. R. (2007). Transitions in early embryonic atrioventricular valvular function correspond with changes in cushion biomechanics that are predictable by tissue composition. *Circ Res, 100*(10), 1503-1511. doi:10.1161/CIRCRESAHA.107.148684

Butcher, J. T., & Nerem, R. M. (2007). Valvular endothelial cells and the mechanoregulation of valvular pathology. *Philos Trans R Soc Lond B Biol Sci, 362*(1484), 1445-1457. doi:10.1098/rstb.2007.2127

Combs, M. D., & Yutzey, K. E. (2009). Heart valve development: regulatory networks in development and disease. *Circ Res, 105*(5), 408-421. doi:10.1161/CIRCRESAHA.109.201566

Coutinho, G. F., & Antunes, M. J. (2017). Mitral valve repair for degenerative mitral valve disease: surgical approach, patient selection and long-term outcomes. *Heart, 103*(21), 1663-1669. doi:10.1136/heartjnl-2016-311031

de Lange, F. J., Moorman, A. F., Anderson, R. H., Manner, J., Soufan, A. T., de Gier-de Vries, C., . . . Christoffels, V. M. (2004). Lineage and morphogenetic analysis of the cardiac valves. *Circ Res, 95*(6), 645-654. doi:10.1161/01.RES.0000141429.13560.cb

de Vlaming, A., Sauls, K., Hajdu, Z., Visconti, R. P., Mehesz, A. N., Levine, R. A., . . . Norris, R. A. (2012). Atrioventricular valve development: new perspectives on an old theme. *Differentiation, 84*(1), 103-116. doi:10.1016/j.diff.2012.04.001

Devereux, R. B., Casale, P. N., Wallerson, D. C., Kligfield, P., Hammond, I. W., Liebson, P. R., . . . Laragh, J. H. (1987). Cost-effectiveness of echocardiography and electrocardiography for detection of left ventricular hypertrophy in patients with systemic hypertension. *Hypertension, 9*(2 Pt 2), II69-76.

Dina, C., Bouatia-Naji, N., Tucker, N., Delling, F. N., Toomer, K., Durst, R., . . . Leducq Transatlantic, M. N. (2015). Genetic association analyses highlight biological pathways underlying mitral valve prolapse. *Nat Genet, 47*(10), 1206-1211. doi:10.1038/ng.3383

Disse, S., Abergel, E., Berrebi, A., Houot, A. M., Le Heuzey, J. Y., Diebold, B., . . . Jeunemaitre, X. (1999). Mapping of a first locus for autosomal dominant myxomatous mitral-valve prolapse to chromosome 16p11.2-p12.1. *Am J Hum Genet, 65*(5), 1242-1251. doi:10.1086/302624

Draghici, S., Khatri, P., Tarca, A. L., Amin, K., Done, A., Voichita, C., . . . Romero, R. (2007). A systems biology approach for pathway level analysis. *Genome Res, 17*(10), 1537-1545. doi:10.1101/gr.6202607

Durst, R., Sauls, K., Peal, D. S., deVlaming, A., Toomer, K., Leyne, M., . . . Slaugenhaupt, S. A. (2015). Mutations in DCHS1 cause mitral valve prolapse. *Nature, 525*(7567), 109-113. doi:10.1038/nature14670

Eisenberg, L. M., & Markwald, R. R. (1995). Molecular regulation of atrioventricular valvuloseptal morphogenesis. *Circ Res, 77*(1), 1-6.

El-Hamamsy, I., Balachandran, K., Yacoub, M. H., Stevens, L. M., Sarathchandra, P., Taylor, P. M., . . . Chester, A. H. (2009). Endothelium-dependent regulation of the mechanical properties of aortic valve cusps. *J Am Coll Cardiol, 53*(16), 1448-1455. doi:10.1016/j.jacc.2008.11.056

Freed, L. A., Levy, D., Levine, R. A., Larson, M. G., Evans, J. C., Fuller, D. L., . . . Benjamin, E. J. (1999). Prevalence and clinical outcome of mitral-valve prolapse. *N Engl J Med, 341*(1), 1-7. doi:10.1056/NEJM199907013410101

Garside, V. C., Chang, A. C., Karsan, A., & Hoodless, P. A. (2013). Co-ordinating Notch, BMP, and TGF-beta signaling during heart valve development. *Cell Mol Life Sci, 70*(16), 2899-2917. doi:10.1007/s00018-012-1197-9

Gherman, A., Davis, E. E., & Katsanis, N. (2006). The ciliary proteome database: an integrated community resource for the genetic and functional dissection of cilia. *Nat Genet, 38*(9), 961-962. doi:10.1038/ng0906-961

Giovanni, A., Capone, F., di Biase, L., Ferreri, F., Florio, L., Guerra, A., . . . Di Lazzaro, V. (2017). Oscillatory Activities in Neurological Disorders of Elderly: Biomarkers to Target for Neuromodulation. *Front Aging Neurosci, 9*, 189. doi:10.3389/fnagi.2017.00189

Grainger, R. J., & Beggs, J. D. (2005). Prp8 protein: at the heart of the spliceosome. *RNA, 11*(5), 533-557. doi:10.1261/rna.2220705

Hartwell, L. H., McLaughlin, C. S., & Warner, J. R. (1970). Identification of ten genes that control ribosome formation in yeast. *Mol Gen Genet, 109*(1), 42-56.

Haycraft, C. J., Zhang, Q., Song, B., Jackson, W. S., Detloff, P. J., Serra, R., & Yoder, B. K. (2007). Intraflagellar transport is essential for endochondral bone formation. *Development, 134*(2), 307-316. doi:10.1242/dev.02732

Hinton, R. B., Jr., Lincoln, J., Deutsch, G. H., Osinska, H., Manning, P. B., Benson, D. W., & Yutzey, K. E. (2006). Extracellular matrix remodeling and organization in

developing and diseased aortic valves. *Circ Res, 98*(11), 1431-1438. doi:10.1161/01.RES.0000224114.65109.4e

Holbrook, K. A., & Byers, P. H. (1989). Skin is a window on heritable disorders of connective tissue. *Am J Med Genet, 34*(1), 105-121. doi:10.1002/ajmg.1320340118

Horne, T. E., VandeKopple, M., Sauls, K., Koenig, S. N., Anstine, L. J., Garg, V., . . . Lincoln, J. (2015). Dynamic Heterogeneity of the Heart Valve Interstitial Cell Population in Mitral Valve Health and Disease. *J Cardiovasc Dev Dis, 2*(3), 214-232. doi:10.3390/jcdd2030214

Kyndt, F., Schott, J. J., Trochu, J. N., Baranger, F., Herbert, O., Scott, V., . . . Benichou, B. (1998). Mapping of X-linked myxomatous valvular dystrophy to chromosome Xq28. *Am J Hum Genet, 62*(3), 627-632. doi:10.1086/301747

Lammers, K., Abeln, B., Husken, M., Lehmacher, C., Psathaki, O. E., Alcorta, E., . . . Paululat, A. (2017). Formation and function of intracardiac valve cells in the Drosophila heart. *J Exp Biol, 220*(Pt 10), 1852-1863. doi:10.1242/jeb.156265

Le Tourneau, T., Merot, J., Rimbert, A., Le Scouarnec, S., Probst, V., Le Marec, H., . . . Schott, J. J. (2018). Genetics of syndromic and non-syndromic mitral valve prolapse. *Heart, 104*(12), 978-984. doi:10.1136/heartjnl-2017-312420

Leask, R. L., Jain, N., & Butany, J. (2003). Endothelium and valvular diseases of the heart. *Microsc Res Tech, 60*(2), 129-137. doi:10.1002/jemt.10251

Lu, H., Toh, M. T., Narasimhan, V., Thamilselvam, S. K., Choksi, S. P., & Roy, S. (2015). A function for the Joubert syndrome protein Arl13b in ciliary membrane extension and ciliary length regulation. *Dev Biol, 397*(2), 225-236. doi:10.1016/j.ydbio.2014.11.009

Makarov, E. M., Makarova, O. V., Urlaub, H., Gentzel, M., Will, C. L., Wilm, M., & Luhrmann, R. (2002). Small nuclear ribonucleoprotein remodeling during catalytic activation of the spliceosome. *Science, 298*(5601), 2205-2208. doi:10.1126/science.1077783

Markwald, R. R., Fitzharris, T. P., Bolender, D. L., & Bernanke, D. H. (1979). Sturctural analysis of cell:matrix association during the morphogenesis of atrioventricular cushion tissue. *Dev Biol, 69*(2), 634-654.

Markwald, R. R., Fitzharris, T. P., & Manasek, F. J. (1977). Structural development of endocardial cushions. *Am J Anat, 148*(1), 85-119. doi:10.1002/aja.1001480108

Masetti, R., Bertuccio, S. N., Astolfi, A., Chiarini, F., Lonetti, A., Indio, V., . . . Pession, A. (2017). Hh/Gli antagonist in acute myeloid leukemia with CBFA2T3-GLIS2 fusion gene. *J Hematol Oncol, 10*(1), 26. doi:10.1186/s13045-017-0396-0

Nauli, S. M., Jin, X., AbouAlaiwi, W. A., El-Jouni, W., Su, X., & Zhou, J. (2013). Non-motile primary cilia as fluid shear stress mechanosensors. *Methods Enzymol, 525*, 1-20. doi:10.1016/B978-0-12-397944-5.00001-8

Person, A. D., Klewer, S. E., & Runyan, R. B. (2005). Cell biology of cardiac cushion development. *Int Rev Cytol, 243*, 287-335. doi:10.1016/S0074-7696(05)43005-3

Rabkin-Aikawa, E., Farber, M., Aikawa, M., & Schoen, F. J. (2004). Dynamic and reversible changes of interstitial cell phenotype during remodeling of cardiac valves. *J Heart Valve Dis, 13*(5), 841-847.

Runyan, R. B., & Markwald, R. R. (1983). Invasion of mesenchyme into three-dimensional collagen gels: a regional and temporal analysis of interaction in embryonic heart tissue. *Dev Biol, 95*(1), 108-114.

Sagie, A., Schwammenthal, E., Newell, J. B., Harrell, L., Joziatis, T. B., Weyman, A. E., . . . Palacios, I. F. (1994). Significant tricuspid regurgitation is a marker for adverse outcome in patients undergoing percutaneous balloon mitral valvuloplasty. *J Am Coll Cardiol, 24*(3), 696-702.

Shrestha, R. K., Ding, P., Jones, J. D. G., & MacLean, D. (2018). A workflow for simplified analysis of ATAC-cap-seq data in R. *Gigascience, 7*(7). doi:10.1093/gigascience/giy080

Spudich, J. A. (2014). Hypertrophic and dilated cardiomyopathy: four decades of basic research on muscle lead to potential therapeutic approaches to these devastating genetic diseases. *Biophys J, 106*(6), 1236-1249. doi:10.1016/j.bpj.2014.02.011

Sultana, N., & Wang, M. (2008). Fabrication of HA/PHBV composite scaffolds through the emulsion freezing/freeze-drying process and characterisation of the scaffolds. *J Mater Sci Mater Med, 19*(7), 2555-2561. doi:10.1007/s10856-007-3214-3

Toomer, K., Sauls, K., Fulmer, D., Guo, L., Moore, K., Glover, J., . . . Norris, R. A. (2019). Filamin-A as a Balance between Erk/Smad Activities During Cardiac Valve Development. *Anat Rec (Hoboken), 302*(1), 117-124. doi:10.1002/ar.23911

Vijayraghavan, U., Company, M., & Abelson, J. (1989). Isolation and characterization of pre-mRNA splicing mutants of Saccharomyces cerevisiae. *Genes Dev, 3*(8), 1206-1216.

Wheway, G., Nazlamova, L., & Hancock, J. T. (2018). Signaling through the Primary Cilium. *Front Cell Dev Biol, 6*, 8. doi:10.3389/fcell.2018.00008

Wheway, G., Schmidts, M., Mans, D. A., Szymanska, K., Nguyen, T. T., Racher, H., . . . Johnson, C. A. (2015). An siRNA-based functional genomics screen for the identification of regulators of ciliogenesis and ciliopathy genes. *Nat Cell Biol, 17*(8), 1074-1087. doi:10.1038/ncb3201